Agricultural and Forest Meteorology 331 (2023) 109309

Contents lists available at ScienceDirect

Agricultural and Forest Meteorology

journal homepage: www.elsevier.com/locate/agrformet

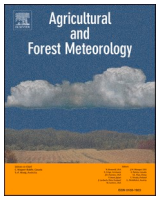

High greenhouse gas emissions after grassland renewal on bog peat soil

Liv Offermanns [a,*], Bärbel Tiemeyer [a], Ullrich Dettmann [a,b], Jeremy Rüffer [a], Dominik Düvel [a], Isabelle Vogel [c], Christian Brümmer [a]

[a] Thünen Institute of Climate-Smart Agriculture, Bundesallee 65, 38116 Braunschweig, Germany
[b] Institute of Soil Science, Leibniz University Hannover, Herrenhäuser Str. 2, 30419 Hannover, Germany
[c] Chamber of Agriculture Lower Saxony, District office Bremervörde, Albrecht-Thaer-Straße 6a, 27432 Bremervörde, Germany

ARTICLE INFO

Keywords:
Submerged drains
Dairy farming
Organic soils
Carbon dioxide
Nitrous oxide
Grassland renovation

ABSTRACT

Drained agriculturally used peatlands are hotspots for greenhouse gas (GHG) emissions, especially carbon dioxide (CO_2) and nitrous oxide (N_2O). To reduce GHG emissions and simultaneously maintain intensive grassland use, raising water levels by subsurface irrigation (SI) is controversially discussed. Both, intensive grassland use and installations of SI may require grassland renewal. We investigated an experimental intervention site (INT) (SI target water levels: -0.30 m) and a deeply drained reference site (REF), both intensive grassland on deep bog peat. After installation of the SI system, a mechanical grassland renewal took place at INT. At both sites, CO_2 (eddy covariance), N_2O and methane (manual closed chamber technique) were measured. Additionally, soil water was analyzed for nitrogen species. Here, we report on the initial year of GHG measurements including grassland renewal and rising water levels. Overall, GHG emissions were strongly influenced by grassland renewal at INT. Despite progressively rising water levels, soil moisture in the upper centimeters was low and thus grass growth was slow, resulting in an almost complete loss of harvest. This resulted in a net ecosystem carbon balance (NECB) of 4.64 ± 1.03 t C ha^{-1} containing only 0.57 ± 0.09 t C ha^{-1} harvest at INT, while NECB at REF was 6.08 ± 1.74 t C ha^{-1} including harvest from five grass cuts. Methane fluxes were negligible at both sites. Nitrous oxide emissions dominated the GHG balance at INT. With 144.5 ± 45.5 kg N_2O–N ha^{-1} a^{-1} they were much higher than at REF (3.9 ± 3.1 kg N_2O–N ha^{-1} a^{-1}) and any other values published so far. Peak fluxes occurred when nitrate concentrations in soil water were extremely high, soil moisture was increased, and vegetation development was struggling. This study highlights the risk of grassland renewals on peat soils regarding yield losses as well as high GHG emissions.

1. Introduction

Intact peatland ecosystems are efficient sinks of atmospheric carbon dioxide (CO_2; Frolking et al., 2006; Frolking and Roulet, 2007). Under water-logged conditions peat is formed due to incomplete decomposition of peat-forming vegetation, and thus carbon is stored for thousands of years (Loisel et al., 2014). It is well known that the water table depth, which is strongly correlated with soil moisture over longer observation periods and thus oxygen availability, has substantial effect on CO_2 emissions (Komulainen et al., 1999; Tiemeyer et al., 2016). Consequently, disturbance, e.g. by drainage to convert peatlands into agricultural land, turns them into strong emitters of CO_2 because mineralization of the organic matter is triggered (Maljanen et al., 2010; Moore and Knowles, 1989).

For European peatlands, Leppelt et al. (2014) estimated that 9–35% is used as grassland. In Germany, 97% of all organic soils are drained, with grassland being the main land-use type (53%; UBA, 2021). Intensity of grassland use in Germany is strongly heterogeneous, ranging from low-intensity grassland managed for meadow birds to highly intensive use in dairy regions. Similar to Germany, peatlands are important for dairy farming in the Netherlands. There is also widespread grassland use in the UK and Ireland, while in many other European regions, croplands or forestry dominate. Overall, drained organic soils in the EU are estimated to emit annually about 220 Mt of CO_2-eq., which comprises 5% of total EU emissions (Tanneberger et al., 2021).

Generally, CO_2 is the most important of all greenhouse gasses (GHG) for grassland on organic soils (IPCC, 2014; Tiemeyer et al., 2016; UBA, 2021). Carbon dioxide emissions frequently increase with decreasing water levels (Evans et al., 2021) although there is indication from laboratory studies that highest respiration rates might occur at

* Corresponding author.
E-mail address: liv@sokolowsky.de (L. Offermanns).

https://doi.org/10.1016/j.agrformet.2023.109309
Received 12 August 2022; Received in revised form 28 October 2022; Accepted 2 January 2023
Available online 25 January 2023

intermediate soil moisture (Kechavarzi et al., 2010; Säurich et al., 2019). Intensity of grassland use, especially the nutrient supply by fertilization, might also play an important role. Nutrient availability influences microbial activity and can increase heterotrophic respiration, but studies have so far mainly been restricted to the laboratory scale (Kechavarzi et al., 2010; Larmola et al., 2013; Säurich et al., 2019).

The second most important GHG emitted from agriculturally used peatlands is nitrous oxide (N_2O; IPCC, 2014; Leppelt et al., 2014; Tiemeyer et al., 2016; UBA, 2021). Dutch and German intensively managed grassland and cropland on organic soils belong to the strongest N_2O emitters in European agriculture (Leppelt et al., 2014). One main reason for these N_2O emissions is a high availability of nitrogen (Repo et al., 2009), especially nitrate. In intensively agriculturally managed peatlands high amounts of nitrate are added through fertilization, however mineralization and nitrification caused by aeration of the peat contribute, too. High nitrate concentrations in the pore water can lead to high denitrification rates which is the major pathway for N_2O production (Butterbach-Bahl et al., 2013; Firestone and Davidson, 1989; Wrage-Mönnig et al., 2018). Prerequisite for denitrification is a soil moisture regime close to saturation corresponding to an intermediate and/or a fluctuating water level (Smith et al., 1998; Tiemeyer et al., 2016; Weslien et al., 2009). The final step of denitrification, i.e. reduction of N_2O to N_2, is pH sensitive (Richardson et al., 2009; Simek and Cooper, 2002) and reported to be hampered by low pH values (van den Heuvel et al., 2011). Low pH values are typical for bog peat, but literature is still inconclusive on the importance of pH values for N_2O emissions (Liimatainen et al., 2018), probably as many factors interact.

Especially at intensively used grasslands, management measures are regularly taken to improve the species composition, yields, or, in case of peat soils, to level surface roughness caused by subsidence. Measures may range from resowing while keeping the entire old grass sward or parts of it to completely destroying the old grass sward by chemical or physical methods (Kayser et al., 2018). In this study, the term "grassland renewal" is used and defined as the mechanical destruction of the entire old sward and resowing of the grass. This belongs to the strongest interventions in a grassland ecosystem with the highest disturbance of the soil and the highest risks of yield losses (Kayser et al., 2018). However, this is the only method which allows for leveling surface roughness. Due to spatially heterogenous subsidence of the peat body, leveling surface roughness from time to time is important for farmers managing grassland on peat. Grassland renewal is limited by European nature conservation legislation and direct payment regulations under the Common Agricultural Policy, but often allowed upon application when necessary for agronomic reasons. With the exception of one study on N_2O only (Buchen et al., 2017), there is no data on the effects of grassland renewal on GHG emissions on peatlands or other organic soils. For mineral soils, a temporary switch from CO_2 sink to source is frequently reported (Ammann et al., 2020; Merbold et al., 2014; Rutledge et al., 2017).

High mineralization rates of soil organic matter in form of the old milled grass sward in course of a mechanical grassland renewal also cause the release of nitrogen (Ammann et al., 2020). This seems to be particularly important for mineral soils with low amounts of organic matter, but might also be relevant for peat soil, because the younger organic matter of the grass sward probably is easier to break down than the peat itself (Bader et al., 2017). Higher nitrogen concentrations in the soil pore water after grassland renewal (Buchen et al., 2017; Velthof et al., 2010) might stimulate N_2O emissions, which has been shown in several studies (Ammann et al., 2020; Krol et al., 2016; Merbold et al., 2014; Velthof et al., 2010) mostly restricted to mineral soils. However, in the above-mentioned study of Buchen et al. (2017) on a Histic Gleysol, only short time responses but no impact on the annual N_2O balance was found.

Rewetting peatlands for ecosystem restoration is a well-proven method to reduce GHG emissions (IPCC, 2014; Wilson et al., 2016). However, a transformation of conventional agriculturally used peatlands towards near-natural conditions is incompatible with dairy farming, especially in regions with a high share of organic soils and thus limited alternative options for fodder production. As long as alternatives for a steady and stable income are not fully developed, taking all peatlands out of agricultural use in the next years or decades is not feasible. Therefore, there is a strong demand for other options taking the needs of farmers into account with regard to productive agricultural land use, but also the urgent need to reduce GHG emissions. Subsurface irrigation (SI; also known as: reverse drainage, submerged irrigation, sub-soil irrigation, submerged drains) has been proposed as a method to achieve higher water levels while keeping an intensive agricultural management (e.g. van den Akker et al., 2012). Narrow-spaced drains are combined with high water levels in ditches, which might be supplemented by groundwater to keep the water table in the peat relatively high in summer, but to ensure drainage in winter and spring (den Hartogh, 2014). The installation of the drains is a major intervention and might thus require grassland renewal or at least resowing afterwards.

Despite being tested for decades (Harris et al., 1962; den Hartogh, 2014), only two field studies with actual GHG measurements on SI sites have been published so far. Weideveld et al. (2021) could not show any clear effect of SI on CO_2, methane (CH_4) or N_2O emissions. However, yearly average water levels were not raised at all and average summer water levels were only slightly higher (0.11 m) than at the control sites. Boonman et al. (2021), though, were able to implement substantially higher water levels. Accordingly, SI resulted in lower CO_2 emissions but also went along with a slight reduction of harvested biomass. Neither N_2O nor CH_4 were included in their study. These results stress the importance of further investigations on SI sites where high water levels could be achieved and all major GHGs are measured.

Our project is the first field-scale study focusing on the evaluation of the effects of subsurface irrigation on greenhouse gas emissions from a peatland under intensive grassland management. We are using the eddy covariance (EC) technique for CO_2 and manual chamber measurements for N_2O and CH_4, accompanied by soil water sampling. Due to installation of the subsurface irrigation system, grassland renewal was necessary at the site (INT). Thus, the initial year of the project was dominated by the impact of strong interventions regarding installation of the SI system and grassland renewal measures, while target water levels (−0.30 m) were only reached after several months. A second deeply drained grassland site under regionally typical management for dairy farming serves as reference site (REF). In this study, we investigated the combined effect of grassland renewal and subsequently raised water levels on CO_2, CH_4 and N_2O emissions as well as on dissolved nitrogen concentrations during one year after grassland renewal.

2. Material and methods

2.1. Study sites and management

We investigated two sites, which have been used as permanent grassland for fodder production over at least the last 30 years within the bog complex "Gnarrenburger Moor" (North-West Germany), with less than 5 km distance to each other. Both sites were intensively managed in the past with 4 to 5 cuts each year, accompanied by high N fertilization rates. The bog complex is located in an intensively managed dairy region and about 80% of its area is nowadays used as grassland. The climate is temperate-oceanic with annual precipitation of 779 mm and mean annual temperature of 9.1 °C (1961–2020; German Meteorological Service, Bremervörde).

2.1.1. Water management

The reference (REF) site (53°24′ N 9°05′ E) is deeply drained with a drain spacing of 8 m and a drainage depth of about 0.7 m. Each drain pipe discharges into deep ditches at the edges of the field.

At the experimental intervention (INT) site (53°22′ N 9°03′ E) a pressurized subsurface irrigation system was installed. "Pressurized" means that the hydraulic gradient is controlled via the water level in a

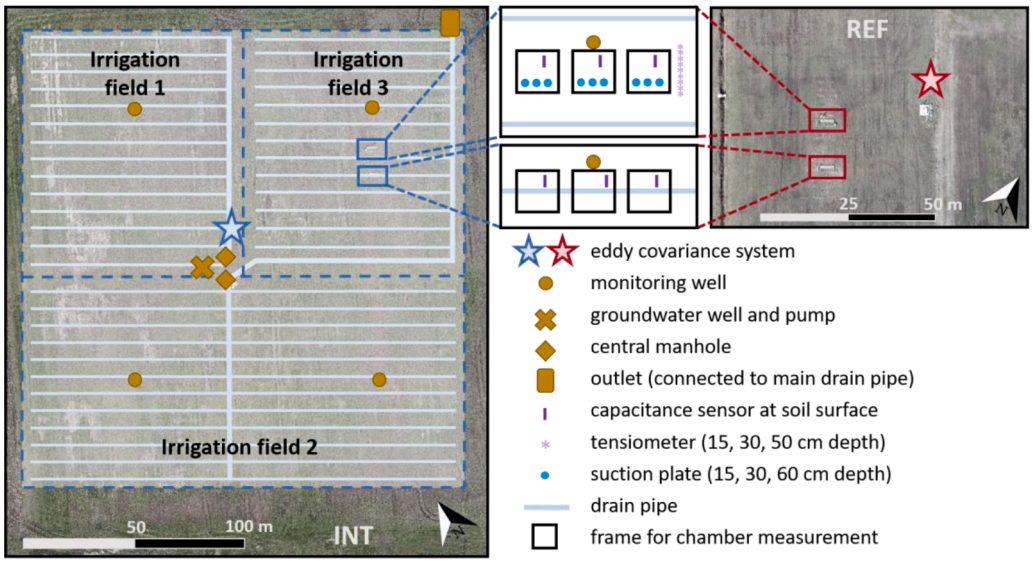

Fig. 1. Schematic illustration of the INT site (left) and a section of the REF site (right) with placement of chamber frames for chamber measurements (middle). Drone pictures were taken on 08.04.2020 (J.-P. Delorme, Thünen Institute). Inserted scales on the drone pictures serve as overall indication of the size of the study site and not for total distances between measurement equipment or drain pipes.

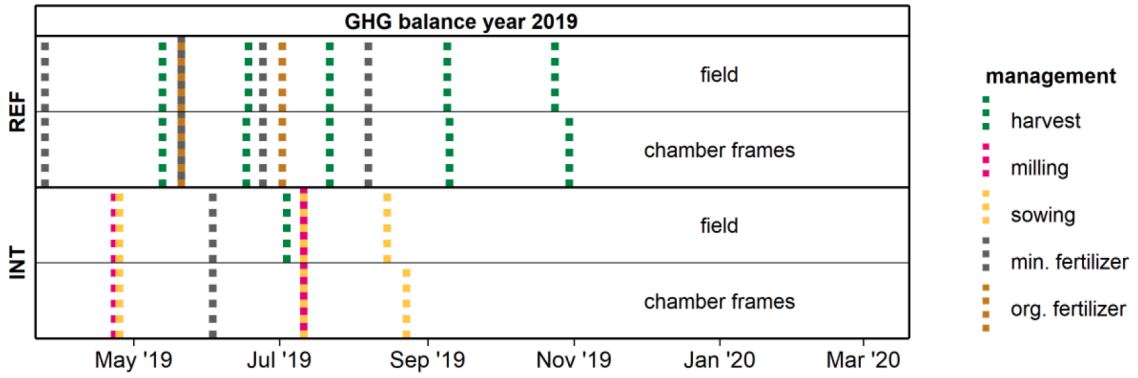

Fig. 2. Illustration of management operations on the field (relating to EC source area for CO_2 measurements) and in chamber frames (relating to N_2O and CH_4 measurements with the chamber technique) at REF and INT. The greenhouse gas (GHG) balance year covers the observation period from 21.03.2019 to 20.03.2020. Besides milling the first measures at SI comprises all interventions of the initial grassland renewal including leveling.

manhole. Therefore, higher hydraulic heads can be used than with subsurface irrigation from ditches, where the head is limited by the lowest part of the ditch banks. The target water level was 0.30 m below soil surface. Drain pipes (4 m spacing) were placed in a depth of 1 m in December 2018. During this process, the existing deeper and wider spaced drain pipes were destroyed. A groundwater well was drilled in March 2019 and equipped with a pump (Lorentz PS2 600 CS-J, max. pump rate: 7.2 m^3 h^{-1}, Henstedt-Ulzburg, Germany) for the water supply using solar power. The pump is controlled by water level sensors in the central manholes and operated from 26.04.2019 to 26.09.2019. The site is divided into three irrigation fields, because the surface elevation is slightly different between these fields. As the water level could be controlled separately for the three irrigation fields, it was possible to apply a homogenous water level depth for the entire site (Fig. 1). The irrigation follows a cascade system: Irrigation field 1 is filled with water first, followed by field 2 and 3. The pressure in each level is controlled by individual overflow pipes in central manholes, while the outlet is also regulated by a flashboard riser. The outlet was closed directly after the grassland renewal (26.04.2019) and opened permanently from 30.09.2019 on, thus excess water in the winter period was released through the main drain pipe into the adjacent ditch.

2.1.2. Grassland renewal and management

Grassland renewal was conducted at the INT site, as the sward was damaged by the placement of the drain pipes. Furthermore, in the course of the renewal the surface was leveled with the intention to implement the same water table depth within each irrigation field. An overview of the management including grassland renewal procedures at the INT site is shown in Fig. 2. In detail, the grassland renewal at the end of April 2019 was done by cutting the grass, then milling the first 10–15 cm to destroy the old grass sward and leveling the field using a snowcat equipped with a leveling blade. However, the leveling helped only marginally to create a more even field, as standard deviation in micro relief was improved by only 1.5 cm (lowest point above sea level: 10.04 m before leveling, 10.05 m after leveling; highest point above sea level: 11.16 m before leveling and 10.87 m after leveling).

After rolling, oat seeds (*Avena sativa*) as well as a grass seed mixture (53% *Lolium perenne*, 20% *Festuca pratensis,* 17% *Phleum pratense*, 10% *Poa pratensis*) were sown and rolling was conducted another two times to ensure good growing conditions. The oat was supposed to suppress unwanted weeds, as it grows faster than grass and can be used as fodder when harvested in an early stage. After a weak development of the grass-oat-mixture, unwanted weeds (abundant e.g. *Polygonum persicaria, Stellaria media, Solanum nigrum;* less abundant e.g. *Cenopodium* spp.)

became dominant in many parts of the field. Additionally, other parts remained bare and an unusually high mice population contributed to the failed grassland development. Consequently, the vegetation was cut and the grassland renewal measures were repeated with milling, rolling and sowing, but without oat seed application or leveling in July 2019.

Meanwhile, the REF site was regularly managed with five harvests and application of organic and mineral fertilizer (Fig. 2). All operations on the field were manually performed inside the frames of the chamber plots.

2.1.3. Vegetation height, biomass export and fertilization

To get information about vegetation development on field scale, representative for the EC footprints, we measured vegetation heights every second week and directly before each harvest. Therefore, 16 randomly distributed points at the REF site and 48 points (16 per irrigation field) at the INT site were used, due to much more heterogeneous growth. For measurements we used a folding rule (5 points within 0.25 m^2 plots; April 2019 to November 2019) and a plate meter (0.25 m^2; November 2019 to April 2020; Op de Beek et al., 2017). In case of the frames for chamber measurements, we additionally measured the vegetation height during each chamber campaign.

At the REF site, we took four randomly distributed biomass samples (0.5 × 0.5 m) inside the EC footprint just before each harvest. Simultaneously, the grass inside the frames used for chamber measurements was harvested. All biomass samples were dried at 60 °C until mass equilibrium to get the dry matter weights (DM). We calculated the mean of all taken samples (field and plots) and used standard error of the mean as uncertainty. For the uncertainty of the total annual harvest at the REF site we used error propagation.

At the INT site no regular harvest took place. Before the second grassland renewal in July the farmer mowed the field but only collected grass and oat plants from areas with low weed abundance and thus adequate fodder quality. Due to the very selective removal of biomass, we could not use the same method to estimate the biomass export as at the REF site. The farmer indicated the amount of harvested fresh matter (estimated number and weight of trailer loads) from which we estimated DM using a mean water content. Uncertainty is given by the standard deviation of the range of collected matter the farmer estimated for us.

Dried field samples taken briefly before each harvest were pooled for each site and analyzed for carbon (C) concentrations (TruMac CN, LECO Corporation, St. Joseph, Michigan, USA) to derive the amount of exported C with the calculated DM and its uncertainties.

Carbon input into the ecosystem from organic fertilization (only REF) was calculated from the amount of cattle slurry the farmer applied and the analysed concentration of total organic C (VDLUFA, 2011). While nitrogen (N), phosphorus (P), and potassium (K) inputs from mineral fertilizer were taken from the manufacturer's declaration, the respective content in organic fertilizer was analysed in the cattle slurry (N: Landwirtschaftliche Untersuchungs- und Forschungsanstalt, LUFA Nord-West in-house method for total N analysis using near-infrared spectroscopy, P and K: DIN EN ISO 11885:2009–09). Total nutrient amounts in applied fertilizer were 230.3 kg N ha^{-1}, 15.4 kg P ha^{-1}, and 104.1 kg K ha^{-1} at REF and 64.8 kg N ha^{-1}, 8.8 kg P ha^{-1}, and 70.1 kg K ha^{-1} at INT.

2.2. Measurement and calculation of GHG fluxes

We used EC systems for measurements of CO_2 at the field scale. For N_2O and CH_4 we used the chamber technique (Fig. 1). We report the GHG balance from 21.03.2019 to 20.03.2020 and use the atmospheric sign convention, i.e. fluxes with a negative sign are defined as uptake by the ecosystem while positive numbers indicate emissions. Calculations of raw CO_2 fluxes were done using the processing software EddyPro (7.0.4. LI-COR Environmental, Lincoln, NE, USA). All further calculations and data handling of half hourly CO_2 fluxes as well as all N_2O and CH_4 flux calculations were done using the R language (R Core Team, 2020).

Table 1
Settings in EddyPro (7.0.4. LI-COR Environmental, Lincoln, NE, USA) for flux calculation.

Processing step	Method used
Axis rotation for tilt correction	Double rotation (Wilczak et al., 2001)
Detrending method	Block average (Gash and Culf, 1996)
Time lag detection and compensation	Covariance maximization (LI-COR, 2022)
Compensation for air density fluctuation	Webb-Pearman-Leuning (Webb et al., 1980)
Low frequency range correction	Analytic correction of high-pass filtering effects (Moncrieff et al., 2004)
High frequency range	Correction of low-pass filtering (Moncrieff et al., 1997)

2.2.1. CO_2 and meteorological measurement systems

Two identical EC setups were placed at the two study sites. The system at the INT site was powered by solar panels and batteries connected to a generator as backup in periods with low solar radiation in winter. The system of the REF site was connected to the public power grid. The measurement height of the Sonic Anemometer (HS-50, Gill, Hampshire, UK) was 2.5 m at both sites. Carbon dioxide concentrations were measured with a LI-7200/RS enclosed path infrared analyzer (LI-COR Environmental, Lincoln, NE, USA) connected to a short heated stainless steel pipe with the inlet closely mounted next to the anemometer transducers. The acquisition rate was 10 Hz. A net radiometer (model CNR4, Kipp & Zonen B.V., Delft, the Netherlands) was used for radiation measurements (global radiation (R_g)) and a Vaisala HMP155A/E sensor (Vaisala, Vantaa, Finland) for air temperature. Air pressure was measured with a Vaisala PTB110 sensor (Vaisala, Vantaa, Finland) at the REF site. Soil temperature was measured with soil temperature profile probes (Th3-s, UMS AG, Munich, Germany) in two replicates close to the EC system at each site (used depth in this study: 5 cm depth). Meteorological data was recorded each minute with a CR3000 (Campbell Scientific Ltd., Logan, UT, USA) logger.

2.2.2. CO_2 flux calculation

2.2.2.1. Raw data processing. We used EddyPro to calculate half-hourly fluxes of CO_2 from high frequency raw data. Table 1 shows standardized and well-established processing and correction settings applied during flux calculation.

2.2.2.2. Quality control of half-hourly CO_2 fluxes. To ensure that turbulent and stationary conditions were given for each calculated half-hourly flux, the flagging policy of 0, 1, 2 after Mauder and Foken (2004) was applied. We only used data flagged as 0 (best quality) or 1 (acceptable quality). We further discarded all half-hourly CO_2 fluxes with a variance > 400 [-] calculated by EddyPro, subsequently repeated identical values for CO_2 molar density or CO_2 mixing ratio as this is a sign of erroneous data processing (R package *openeddy*, Šigut, 2021), and fluxes with an average signal strength of the LI-7200/RS < 75%. Friction velocity (u_*) thresholds were estimated for each site to find periods with low turbulent mixing using the R package *REddyProc* (Wutzler et al., 2020) presented in Wutzler et al. (2018). Afterwards, all remaining negative nighttime NEE fluxes were rejected as plants favoring CAM photosynthesis could be excluded at our sites.

Finally, half-hourly CO_2 flux spikes were filtered, using a MAD (median of absolute deviation) based approach (Mauder et al., 2013; Papale et al., 2006). The dataset was divided into nighttime ($R_g \leq 10$ W m^{-2}) and daytime fluxes ($R_g > 10$ W m^{-2}). We compared each value with its direct neighbors as: $d_i = (v_i - v_{i-1}) - (v_{i+1} - v_i)$ for 13-day blocks of consecutive records. Block length was limited to < 13 days in the occurrence of either harvest or grassland renewal. Whenever v_{i-1}

or v_{i+1} was missing, these values were replaced by the median of the data block. Additionally, at the beginning and end of each nighttime data block one daytime NEE value was added in order to calculate the d_i value for each half hour. Likewise, a nighttime NEE value was added at the beginning and end of each daytime data block. The MAD was calculated as $MAD = median\ (|d_i - Md|)$ with Md being the median of the differences d_i. NEE was defined as spike whenever: $d_i < Md - \left(\frac{z * MAD}{0.6745}\right)$ or $d_i > Md + \left(\frac{z * MAD}{0.6745}\right)$. We chose a z value of 7 which is one of the more conservatively used values and found 83 spikes for REF and 146 for INT.

2.2.2.3. Gap filling. Short gaps up to one hour in air and soil temperature and R_g were filled using linear interpolation. Longer periods of unavailable site data were filled with data from the other site using a linear regression for a short period just before and after the respective gap. Negative values for R_g were set to 0 W m^{-2}.

To fill missing half-hourly CO_2 fluxes (gap size INT: 32%, REF: 39%) with average CO_2 fluxes occurring under similar meteorological conditions, we used a Look-Up table (*REddyProc*) with five variables and respective tolerances: R_g (5 W m^{-2}), vapor pressure deficit (VPD; 5 hPa), soil temperature (2.5 °C), vegetation height (5 cm), and water level (10 cm). We started with all five variables, left out one of them step by step (order: water level, soil temperature, VPD) and ran each step with different window sizes, always beginning with a window of 1 day and not exceeding a window size of 11 days. We could fill the major number of gaps using all five variables with a window size up to 3 days already (remaining gap size INT: 9%, REF: 4%) and remaining gaps were filled with larger window sizes and/or less variables. With the dataset free of gaps, annual NEE budgets could simply be calculated by summarizing all half-hourly fluxes.

2.2.2.4. Partitioning NEE into GPP and R_{eco}. The measured CO_2 flux is assumed to represent the net ecosystem exchange (NEE) ignoring CO_2 storage in the air masses underneath the sensor height, plus horizontal and/or vertical advection (Aubinet et al., 1999) as these terms are either cancelling each other out when averaging over sufficiently long periods or cannot be measured with a single site tower. NEE is the difference between gross primary production (GPP), constituting carbon uptake through photosynthesis, and carbon release through respiration of the ecosystem (R_{eco}). For partitioning NEE into GPP and R_{eco} we used the nighttime method by Reichstein et al. (2005) implemented in *REddyProc*. Nighttime data were defined by $R_g < 10$ W m^{-2}. Gross primary production is calculated subsequently as R_{eco} minus NEE.

2.2.2.5. Uncertainty estimation. The EC sampling error is taken into account by calculating the random uncertainty after Finkelstein and Sims (2001). Additionally the bias error resulting from gap filling was accounted for by calculating the standard deviation of binned fluxes under similar meteorological conditions (Wutzler et al., 2018).

For calculation of uncertainties for cumulative sums, we used error propagation for the half-hourly random error, when the respective flux was not filled and simply added the bias error when a flux was filled, following Moffat et al. (2007) and Lucas-Moffat et al. (2018). The last estimated error of the cumulative timeline was used as error for annual balances.

2.2.2.6. Footprint analysis. Footprints of the EC systems were calculated for each site based on the whole observation period in order to check for the homogeneity of the source areas of the measured CO_2 fluxes. We followed the approach of Kljun et al. (2015) using the *calc_footprint_FFP_climatology* R function (https://footprint.kljun.net, last change in code: 25.03.2018). The approach is based on a two dimensional parametrization for flux footprint predictions using the Lagrangian stochastic particle dispersion model LPDM-B (Kljun et al., 2002).

2.2.3. N_2O and CH_4 measurements

Depending on season, on drained peatland sites the water table between two drains has either a convex or concave shape. In order to cover the whole range of water table depths at both study sites, we placed three PVC frames directly on a drainage pipe and three frames in the middle between two drain pipes (Fig. 1). They were installed by cutting into the first centimeters of the peat and pushing them into the ground. With the exceptions of the first grassland renewal at the INT site, during which the frames were removed, they remained permanently at the field sites. All other management procedures the farmers conducted on the fields were imitated manually in each individual frame.

We used opaque static ventilated and vented chambers (0.78 m x 0.78 m x 0.50 m) in biweekly campaigns with additional measurements 1, 3, and 7 days after soil tillage or fertilization. When fertilization was conducted only at one of the sites, the higher flux measurement frequency was applied at the other site as well. To ensure airtightness, chambers had rubber seals and were fastened to the frames with 4 clamps each. During the campaigns, semiautomatic sampling devices were connected with tubes to the chambers. Five gas samples within 80 min, with the first sample taken directly after placing the chamber on a frame, were taken (details in Oestmann et al., 2022). Concentrations of CO_2, N_2O and CH_4 were determined by a gas chromatograph (GC-2014 Gaschromatograph, Shimadzu, Kyoto, Japan). Samples with high N_2O concentration (> 10 ppm) were additionally measured with a 7890A Gaschromatograph (Agilent, Santa Clara, CA, USA).

2.2.4. N_2O and CH_4 flux calculation

2.2.4.1. Quality check. Processing of measured gas concentrations and calculation of N_2O and CH_4 fluxes were conducted identically to Oestmann et al. (2022). As CO_2 uptake in opaque chambers is implausible, data points with CO_2 concentrations more than 10 ppm lower than those of the previous sample point showed leakage or sample mix-up. The corresponding N_2O and CH_4 measurement of the same sample were omitted of further calculations. If two of the five samples of a chamber measurement were identified as outliers, the whole flux measurement was discarded. In the period from 17.04.2019 to 03.07.2019 (38% of the measurement campaigns) we observed occasional malfunctioning of the sampling devices (sometimes valves were not switching due to moisture), but otherwise robust and plausible concentration data, thereby allowing flux calculation based on only three gas samples.

2.2.4.2. Flux calculation. Fluxes were calculated with robust linear (RL) or Hutchinson-Mosier regressions (HMR, Pedersen et al., 2010) using the R package *gasfluxes* (Fuß, 2020). The decision between RL and HMR was done based on the kappa.max approach as described in Hüppi et al. (2018), which accounts for bias and uncertainty depending on the accuracy of the GC measurement and the measurement time. In addition, calculated N_2O and CH_4 fluxes were discarded, if the CO_2 flux of the same samples were less than 30% of the maximum CO_2 flux of the other two replicates at the same measurement site. At the REF site N_2O fluxes were calculated with RL in 88% and with HMR in 6% and CH_4 fluxes with RL in 92% and with HMR in 2% of all cases. At the INT site N_2O fluxes were calculated with RL in 52% and with HMR in 42% and CH_4 fluxes with RL in 93% and with HMR in 1% of all cases. No N_2O and CH_4 flux could be calculated in 6% at both sites and for both gasses.

2.2.4.3. Annual balance and uncertainty estimation. To estimate annual balances and their uncertainties of N_2O and CH_4 we used the same approach as in Oestmann et al. (2022) and Günther et al. (2015). We generated 2000 time series, randomly using one of the three replicates of a site for each measurement day. For each of the time series one measurement day was left out (jack-knife method) and the remaining measurements were used to calculate annual balances by linear interpolation. For each measurement site, the annual flux estimate is

Table 2
Profile information at the sites for chamber measurements at the REF and INT site. Total peat depth at REF: > 240 cm and at INT: 322 cm. Horizon information of total nitrogen (TN), total carbon (TC) and their ratio (C:N), pH, phosphorus (P), potassium (K), bulk density (BD), and porosity (ϵ) are shown until a depth of 1 m. For BD and ϵ mean and ± standard deviations are calculated from six replicated samples.

site	location	horizon depth *[cm]*	peat type	von Post	TN *[%]*	TC *[%]*	C:N	pH	P *[mg cm^{-3}]*	K *>[mg cm^{-3}]*	BD *[g cm^{-3}]*	ϵ *[cm^3 cm^{-3}]*
REF	between drains	0–5	amorphous peat	H10	1.80	33.2	18.5	4.4	0.04	0.10	0.36 ± 0.03	0.87 ± 0.01
		5–22	*Sphagnum* peat	H2	0.89	43.1	48.4	3.9	0.00	0.01	0.11 ± 0.00	0.95 ± 0.02
		22–43	*Sphagnum* peat	H3	0.81	47.3	58.4	3.6	0.00	0.01	0.10 ± 0.00	0.96 ± 0.01
		43–63	*Sphagnum* peat	H3	0.96	48.3	50.3	3.4	0.00	0.02	0.10 ± 0.01	0.96 ± 0.00
		63–68	*Sphagnum* peat	H2	0.60	46.0	76.7	3.4	0.00	0.02	–	–
		68–77	*Sphagnum* peat	H6	0.98	49.2	50.2	3.4	0.00	0.02	0.11 ± 0.00	0.96 ± 0.01
		77–117	*Sphagnum* peat	H4	0.83	48.2	58.0	3.5	0.00	0.02	0.08 ± 0.00	0.96 ± 0.00
REF	on a drain pipe	0–20	*Sphagnum* peat	H5	0.60	45.2	75.3	3.7	0.00	0.02	0.12 ± 0.01	0.95 ± 0.00
		20–65	*Sphagnum* peat	H2	0.78	46.4	59.4	3.4	0.00	0.01	0.10 ± 0.01	0.96 ± 0.01
		65–85	*Sphagnum* peat	H3	0.98	48.4	49.4	3.4	0.00	0.03	0.10 ± 0.01	0.95 ± 0.00
		85–140	*Sphagnum* peat	H5	1.25	49.0	39.2	3.5	0.00	0.03	0.11 ± 0.00	0.96 ± 0.00
INT	between drains	0–20	amorphous peat	H10	2.05	43.5	21.2	4.2	0.02	0.06	0.21 ± 0.01	0.87 ± 0.01
		20–53	*Sphagnum* peat	H2	0.72	46.3	64.3	3.7	0.00	0.00	0.13 ± 0.06	0.91 ± 0.02
		53–92	*Sphagnum* peat	H3	0.83	46.8	56.4	3.7	0.00	0.01	0.09 ± 0.01	0.94 ± 0.02
		92–105	*Sphagnum* peat	H5	1.29	49.7	38.5	3.7	0.01	0.01	0.10 ± 0.01	0.97 ± 0.00
INT	on a drain pipe	0–17	amorphous peat	H10	2.08	41.1	19.7	4.4	0.02	0.03	0.30 ± 0.02	0.85 ± 0.01
		17–33	*Sphagnum* peat	H4	0.90	47.1	52.4	4.2	0.01	0.00	0.13 ± 0.02	0.94 ± 0.01
		33–70	*Sphagnum* peat	H3	0.97	44.5	45.8	3.9	0.00	0.01	0.10 ± 0.01	0.95 ± 0.00
		70–117	*Sphagnum* peat	H2	0.82	47.2	57.5	3.8	0.00	0.01	0.07 ± 0.00	0.89 ± 0.01

given by the mean of the jack-knife means and the error by the mean of all jack-knife errors.

2.2.5. Net ecosystem carbon and greenhouse gas balance

The net ecosystem carbon balance (NECB) in t C ha^{-1} a^{-1} is calculated as follows: $NECB = NEE + CH_4 - C_{in} + C_{out}$, with C_{in} being C input from seeds and fertilization and C_{out} the carbon exported *via* harvested material. For the annual GHG balance we converted N_2O and CH_4 to CO_2-eq. with respect to their global warming potential compared to CO_2 within the next 100 years, which is 265 and 28, respectively (Myhre et al., 2013, IPCC Fifth Assessment Report). The total GHG balance in t CO_2-eq. ha^{-1} a^{-1} was calculated using the following equation: $GHG = NEE + 265\ N_2O + 28\ CH_4 - C_{in} + C_{out}$. C_{in} and C_{out} were converted to CO_2. Fluvial losses of carbon are potentially an important component of the NECB, but their determination was beyond the scope of this study. Uncertainties for NECB and the GHG balance were calculated by error propagation.

2.3. Soil hydro-meteorological data and peat properties

2.3.1. Soil properties

Close to the frames for chamber measurements, soil profiles were dug to characterize the horizons (Table 2). At the INT site both profiles were dug after the grassland renewal had already been conducted. Peat type and the degree of decomposition according to the von Post scale from H1 (not decomposed) to H10 (highest degree of decomposition) were determined according to Ad-Hoc-AG Boden (2005) in the field. For physical and chemical analyses soil samples were taken to the lab and cooled (5 °C) until analyses. All peat profiles were classified as Ombric Drainic Fibric Histosols (Hyperorganic; IUSS Working Group WRB, 2015) or "Normerdhochmoor" according to the German classification (Ad-Hoc-AG Boden, 2005). A more detailed comparison of the two profiles is presented in *Section 3.1 Weather conditions and study sites*.

Mixed samples from each horizon were taken and homogenized with a knife mill (Knife Mill GRINDOMIX GM 300, Retsch® GmbH, Haan, Germany) before subsamples were taken for different analyses. One subsample was dried at 105 °C and milled for total C and N analysis via dry combustion (TruMac CN, LECO Corporation, St. Joseph, Michigan, USA). The easily available P and K contents were determined in a second subsample using a calcium acetate lactate extract following VDLUFA (2012). The concentrations in the filtered suspension were determined using an emission spectrometer with coupled plasma (ICP-OES, iCAP 7400 Thermo Fisher Scientific, Waltham, Massachusetts, USA). A third subsample was extracted with a 0.01 mol L^{-1} $CaCl_2$ solution for subsequent pH measurement following DIN ISO 10390:2005-12 (pH electrode: Blue Line 28 pH, SI Analytics, Mainz, Germany).

Additionally, six undisturbed sampling rings were taken for calculation of bulk density (BD) and saturated water content (equivalent to porosity (ϵ)) using dry mass and saturated weight, respectively.

2.3.2. Water table depth

We installed slotted PVC pipes with a continuously logging pressure sensor (Mini-Diver, Eijkelkamp Soil & Water, Giesbeek; the Netherlands) at the middle of each set of three frames for chamber measurements (Fig. 1). For atmospheric pressure corrections, we used the air pressure sensor at the REF site. The pipes were anchored in the underlying mineral substrate to avoid movements with the peat. To account for surface motion, we measured the distance between ground surface and the top of the dipwell twice a month, interpolated these values and used them to derive water table depths from the pressure data.

Due to the simple drainage network design at the REF site, the whole range of water levels should be captured with these two monitoring wells directly at and in the middle between two drain pipes. Thus, the mean water level represents the average water level of the site.

SI had different water management levels (Fig. 1), which – despite all efforts for a uniform water table depth across the whole field – showed some differences. Additional wells and pressure sensors (Rugged TROLL 100, In-Situ, Fort Collins, CO, USA) were placed in 1 m distance to a drain pipe and thus should show an average water level for the respective part of the field. Combining the information from a digital elevation model, the daily mean water level depth in each irrigation field and the daily EC footprint analysis (see *Section 2.2.2.6 Footprint analysis*), we assigned an average water level to the source area of the EC fluxes. The elevation model was generated from surface measurements in May 2019 and March 2020 and an interpolation in between.

2.3.3. Soil hydrology

Additional to water levels we measured soil hydrological parameters. Tensiometers (T8, ecoTech Umwelt-Meßsysteme GmbH, Bonn, Germany) were placed next to a set of three frames between two drain pipes in 15, 30 and 50 cm depth at each site to measure suction of soil water.

The dielectric constant was measured by capacitance sensors (GS3, Meter Group, Pullman, WA, USA), which were inserted from top into the

Table 3
Mean and standard deviation of water levels as well as water filled pore space (WFPS) and soil water content (SWC) in 0–5 and 15 cm depth within the whole balance year and during summer (01.05. – 31.10.2019). "Between drains" and "on a drain pipe" indicates that measurements took place at the locations of the chamber frames for chamber measurements.

site	location	water level	summer water level	WFPS 0–5 cm depth	summer WFPS	SWC 0–5 cm depth	summer SWC
		[m]	*[m]*	*[-]*	*[-]*	*[cm^3 cm^{-3}]*	*[cm^3 cm^{-3}]*
REF	field	−0.82 ± 0.27	−1.05 ± 0.13				
	between drains	−0.72 ± 0.32	−0.99 ± 0.18	0.45 ± 0.15	0.33 ± 0.09	0.40 ± 0.13	0.29 ± 0.08
	on a drain pipe	−0.93 ± 0.23	−1.11 ± 0.10	0.49 ± 0.14	0.39 ± 0.12	0.46 ± 0.13	0.37 ± 0.12
INT	EC footprint-average	−0.24 ± 0.16	−0.30 ± 0.17				
	field	−0.26 ± 0.16	−0.33 ± 0.17				
	irrigation field 1	−0.22 ± 0.21	−0.34 ± 0.17				
	irrigation field 2	−0.20 ± 0.11	−0.23 ± 0.13				
	irrigation field 3	−0.39 ± 0.15	−0.43 ± 0.17				
	between drains	−0.59 ± 0.25	−0.66 ± 0. 29	0.50 ± 0.12	0.44 ± 0.12	0.43 ± 0.10	0.38 ± 0.10
	on a drain pipe	−0.46 ± 0.22	−0.44 ± 0.20	0.49 ± 0.12	0.44 ± 0.12	0.45 ± 0.12	0.41 ± 0.11

soil in each frame (Fig. 1). Soil water contents (SWC) were calculated with the measured dielectric constants and bulk densities of the respective soil horizons, following Malicki et al. (1996). Gap filling was performed with a hydrological Model (Hydrus 1D; Šimůnek et al., 2013). The model was set-up for each individual plot using a soil profile of 1.5 m, with an element refinement towards the top. The top boundary condition was set to atmospheric using precipitation and potential evaporation from the weather station in Bremervörde (operated by the German Meteorological Service). As bottom boundary condition, the water table readings of the sites were set as variable pressure heads. Parameters of a bimodal van Genuchten-Mualem model (Durner, 1994; Mualem, 1976; Priesack and Durner, 2006; van Genuchten, 1980) were optimized by minimizing the residual sum of squares of measured and simulated SWC. Achieved root mean square errors were low (SWC 2 – 6%).

Water filled pore space (WFPS) was calculated by dividing SWC by the highest available SWC of the timeline (including data until May 2021). We also compared the respective maximum SWC to measurements of saturated water content (equivalent to porosity) at undisturbed sampling rings (Table 2) from those horizons where the capacitance sensors were placed and used these values for WFPS calculation if they were higher than maximal SWC values. This was the case at the REF site, as no water logged conditions occurred at the soil surface. For the INT site maximum SWC were comparable or higher than measurements at sampling rings.

2.4. Soil water sampling and analysis

Soil water was sampled with borosilicate glass suction plates (eco-Tech Umwelt-Meßsysteme GmbH, Bonn, Germany) under the frames for chamber measurements between two drain pipes. Under each frame, suction plates in 15, 30 and 60 cm were installed and connected to glass bottles using Teflon tubes (Fig. 1). Negative pressure in the glass bottles was set individually for each depth depending on the current tensiometer readings and collected soil water was taken approximately every second week. For dissolved organic carbon (DOC) analysis samples were stored cooled (4 °C), the remaining water was stored at −20 °C and thawed for analyzing dissolved inorganic nitrogen (DIN; nitrate (NO_3^-), ammonium (NH_4^+)) and total dissolved nitrogen (TDN). Analysis of DOC was done with a Dimatoc 2000 (Dimatec Analysentechnik, Essen, Germany), DIN was analyzed with an ion chromatograph (Metrom, Filderstadt, Germany) and TDN with a total nitrogen analyzer (TN-100, Mitsubishi Chemical Analytech, Kanagawa, Japan). Subsequently, dissolved organic nitrogen (DON) was determined by subtracting DIN from TDN. Analytical problems are common for high DIN:TDN ratios. Graeber et al. (2012), for example, found large errors for samples with DIN:TDN ratios larger than 0.6 using a similar analytical approach as in this study. This threshold is exceeded in many cases in our study, sometimes resulting in negative DON values. We used a linear regression between DON and DOC to estimate plausible DON (and thus TDN) concentrations for samples with high DIN values (R^2 REF: 0.93, R^2 INT: 0.94). For the INT site, almost only soil water from 60 cm depth could be used for the correction, as DIN concentrations mostly were too high in 15 and 30 cm.

3. Results and discussion

3.1. Weather conditions and study sites

Annual precipitation (757 mm, weather station in Bremervörde operated by the German Meteorological Service) was slightly lower and mean air temperature (10.5 °C) more than 1 °C higher than the long-term average from 1961 to 2020. In addition to the weather conditions of our study periods and the water management, water levels and soil moisture were still influenced by the drought year 2018, which had led to unusually low water levels in winter and spring 2019.

As the two investigated sites are located in the same peat complex, less than 5 km apart from each other, the historical use as well as the recent management intensity are equal, thereby assuring a good comparability. This is demonstrated by similar soil profile characteristics, soil physical and chemical properties (Table 2). However, the upper soil differs between the two sites, which is a result from the time of sampling. The soil profiles were dug after the mechanical grassland renewal was conducted at INT, thus the upper 15 cm are strongly disturbed and cannot be compared to the REF site. Below, the *Sphagnum* peat was waekly decomposed (first H2 - H4, in greater depth also up to H6), C:N ratios were wider (38.5–76.7) and pH values mostly lower (3.4–4.2) at both sites. Bulk density was higher in the upper layer (up to 0.36 g cm^{-3}) as compared to deeper layers (around 0.1 g cm^{-3}).

Water levels at the REF site showed a typical seasonal pattern of drained peatlands with lowest values (minimum −1.26 m; Table 3) in September and higher, more fluctuating values in winter (Fig. 3, Fig. 4). Mean annual water level was at −0.82 ± 0.27 m (Table 3). Water filled pore space showed a pattern similar to the peat water levels (Fig. 5).

Initially, water levels within the average daily footprint of the EC system at the INT site were as low as at the REF site. From May 2019 onwards, they showed a completely different pattern, reaching target water levels in September. This resulted in a higher mean annual water level (−0.24 ± 0.16 m; Table 3) and a difference of 0.75 m for mean summer water levels between the two sites. The rising water levels in summer in the observed first year of irrigation clearly show that the subsurface irrigation system technically works well and might perform even better in the next years when water can already be held back in spring by closing the outlet. The water level curve at INT (Fig. 3, Fig. 4) seems to be fluctuating much more than at the REF site, but this is the result of the spatial heterogeneity and water levels of the different irrigation fields and the assignment of these water levels to the daily EC source areas. Depending on the location and extent of the EC footprint,

the water table depth within the footprint might change from day to day even if the water level was stable within the different irrigation fields.

Until June, WFPS in the upper soil at the INT site was similar to the REF site, after that it was at a constant level, whereas it decreased at the REF site until August (Fig. 5). Water levels in summer at the INT site were around 20 cm higher directly on a drain pipe as compared to the middle between two drain pipes, but in the course of the summer still higher than at the REF site. Patterns of WFPS at INT were mostly similar to the REF site, but when the water level was high at INT, WFPS showed much stronger spikes.

3.2. CO_2 fluxes and net ecosystem carbon balance

Prior to the first grassland renewal at the INT site, NEE was not equal at the two sites due to very divergent circumstances. At INT, NEE was close to zero, whereas at the REF site CO_2 uptake occurred. Respiration was similar at both sites, thus the reason for the difference in NEE was the lower GPP at the INT site. A lower productivity at INT probably came from a lower nutrient availability, as the REF site had been fertilized once prior to the beginning of the balance year (org. fertilizer: 04.02.2019) and another time just after the beginning of the balance year (min. fertilizer: 25.03.2019), whereas no fertilization took place at the INT site. We do not have field water levels prior to the grassland renewal at the INT site, but WFPS in the upper centimeters was comparable at the chamber frames at both sites.

3.2.1. Pattern of CO_2 fluxes REF

The pattern of NEE, R_{eco} and GPP differed strongly between the two sites (Fig. 3). At the REF site, the CO_2 flux patterns represent a typical annual course for grassland on peat with strong reactions to harvest events. At the beginning of the balance year (March to June), we saw high GPP rates while R_{eco} was rather small compared to the upcoming months, resulting in predominantly net CO_2 uptake around this time. Especially before the first harvest, almost only net CO_2 uptake occurred for daily fluxes, which fits well to a typically high export of biomass with the first harvest and with this, the temporary stored carbon (0.9 ± 0.1 t C ha^{-1}). After each harvest, at least for several days, daily CO_2 fluxes remained positive, because the grass was short and CO_2 uptake through photosynthesis could not exceed CO_2 emission from respiration. After the second harvest, almost no daily net CO_2 uptake occurred for the rest of the balance year. In the course of the summer, smaller GPP probably resulted from an increasing limitation of photosynthesis due to insufficient water availability as the water levels decreased continuously. This assumption fits to findings of Fu et al. (2022), who calculated a critical soil moisture threshold of $27 \pm 10.6\%$ SWC for two temperate grasslands by investigating the covariance between VPD and GPP on an ICOS (Integrated Carbon Observation System network of eddy covariance observations) dataset. At the REF site SWC between two drain pipes was lower than this threshold until the beginning of October (mean SWC from second harvest to 1.10.2019: 24%) and SWC on a drain pipe (mean SWC from second harvest to 1.10.2019: 30%) was within the estimated uncertainty. One more factor might be a growing mice population in the course of the year 2019, resulting in damage of the grass cover and thus a decrease in GPP, still there were three other harvests possible. At the same time, mean daily temperatures were high, causing high decomposition rates reflected in high R_{eco} rates. The strong influence of temperature on R_{eco} is already well investigated (Boonman et al., 2021; D'Angelo et al., 2016; Juszczak et al., 2013; Lafleur et al., 2005; Tuittila et al., 2004).

3.2.2. Pattern of CO_2 fluxes at INT – effects of and problems with the grassland renewal

At the beginning of the study period, patterns of CO_2 fluxes at the INT site were strongly influenced by the grassland renewal with repeated milling, but raised water levels increasingly gained in influence. Distinct changes in NEE, GPP and R_{eco} occur after milling the upper 10–15 cm of soil to destroy the old grass sward in April and the weeds in July. After each of these strong interferences NEE stayed at a level of about 5 g C m^{-2} d^{-1} for several days.

Overall, the grassland renewal did not work as planned as grass growth remained poor and almost no grass could be harvested. After the first renewal operations, upcoming weeds increased daily GPP until these were cut in July. During that time, daily GPP and R_{eco} reached highest values at the INT site of the entire balance year. In contrast, at the REF site R_{eco} drops down strongly in June and begins to raise again in July. There are several possible reasons for the increased R_{eco} and GPP at INT. First, the peat had been disturbed during the renewal procedure and fresh grass and root biomass was available for decomposition. Both, increasing temperature and water table depth might provide favourable conditions for microorganisms. Intermediate water levels were found to hold optimum conditions for heterotrophic respiration reported in lab studies (Kechavarzi et al., 2010; Säurich et al., 2019). Second, immediately before the increase of CO_2 emissions in June, a fertilizer application with high amounts of N (64.8 kg ha^{-1}), P (8.8 kg ha^{-1}) and K (70.1 kg ha^{-1}) took place, which promoted the growth of unwanted weeds more than growth of seeded species. High N, P, and K availabilities are not only increasing GPP due to stronger plant growth but are also reported to increase R_{eco} (Larmola et al., 2013; Säurich et al., 2019). Finally, another beneficial factor for increasing plant (mainly unwanted weeds) growth might have been increasing soil moisture from consecutive precipitation days. Only marginal changes in soil moisture in the upper centimeters were detectable at the chamber measurement frames, but water table and soil moisture are heterogenous (Fig. 3, Fig. 5). Additionally, the fast growing unwanted weeds might have profited from the already risen water levels, which their roots might have reached already or soil moisture was higher in other parts of the field. Higher temperatures and longer daylight at this time of the year probably promoted their growth as well.

Overall, grass growth was strongly hampered by water stress, which could not significantly be decreased in the upper centimeters by subsoil irrigation due to limited capillary rise in summer in large parts of the field. Comparing to the threshold of SWC for water stress in temperate grassland ($27 \pm 10.6\%$) determined by Fu et al. (2022) SWC at the INT site was mostly above the threshold median but still within the given uncertainty range until mid of August (mean SWC from grassland renewal until 15.08.2019: 32% (plots between two drain pipes) and 33% (plots on a drain pipe)). Further, in contrast to REF where soil moisture was even lower in summer, there were no deep grass roots of an established grass sward which could access water in deeper horizons. The water stress was presumably not only due to meteorological conditions but also intensified by the grassland renewal, with aeration of the upper peat layer and destruction of soil structure. Even when grass growth could be established at adequate water levels in September, single larger patches still remained free of vegetation until March 2020. Besides the unfavorable weather conditions, the patchy grass growth might be traced back to leveling the field, where deeper peat horizons came to the surface. This well-preserved *Sphagnum* peat is much poorer in nutrients and lower in pH than the upper few centimeters of the peat (Table 2), which might hamper the cultivation of grass (or even other unwanted weeds). Overall, despite the leveling procedure, water table

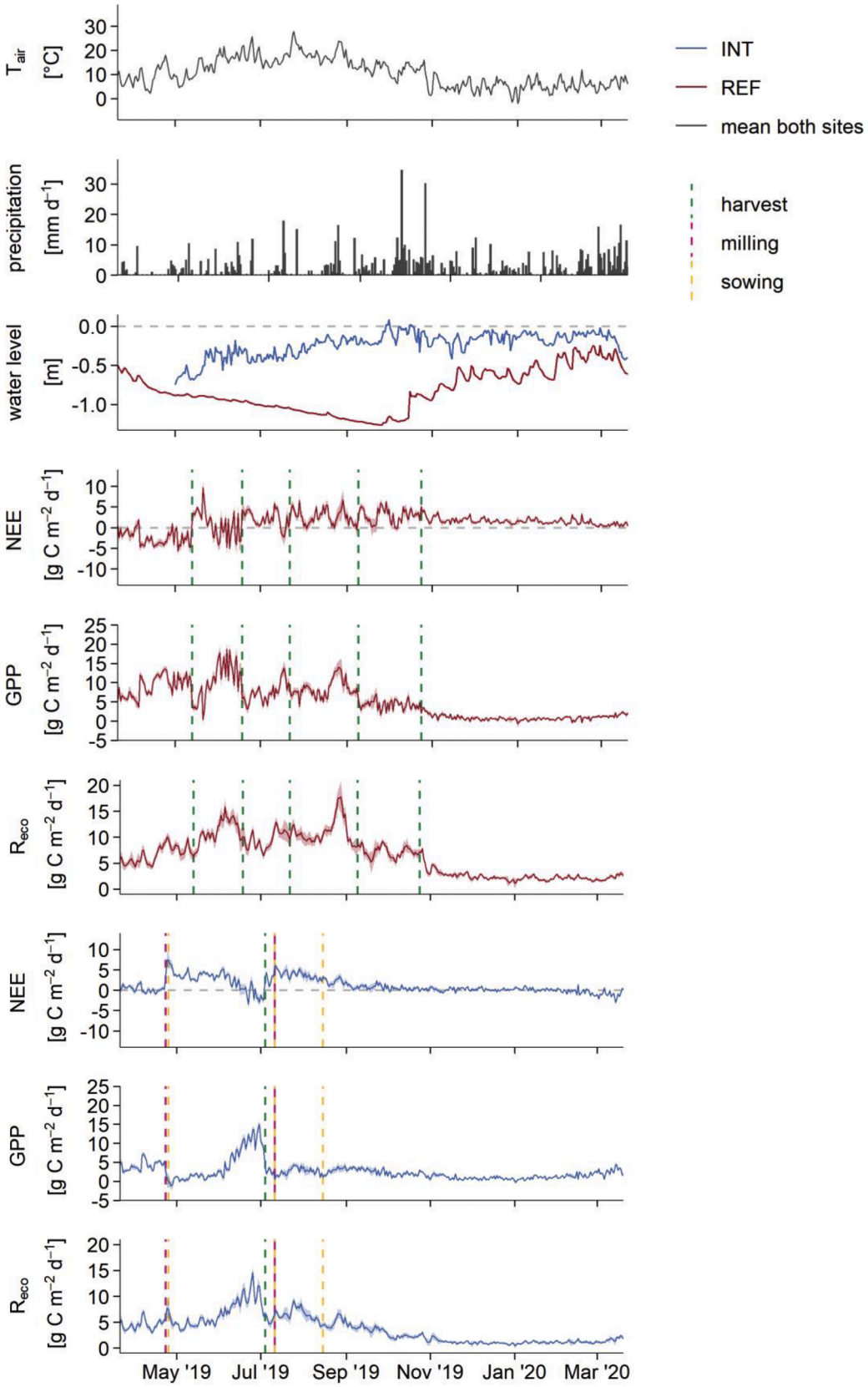

Fig. 3. Mean daily air temperature (T_{air}; mean of both eddy covariance stations), sum of daily precipitation (weather station in Bremervörde operated by the German Meteorological Service), mean daily water levels and daily CO_2-fluxes shown as net ecosystem exchange (NEE) and partitioned into gross primary production (GPP) and respiration of the ecosystem (R_{eco}) at both sites.

Table 4
Mean annual emissions and uncertainties of net ecosystem exchange (NEE), nitrous oxide (N_2O), methane (CH_4), harvest and inputs in form of applicated seeds and fertilization, net ecosystem carbon balance (NECB) and greenhouse gas (GHG) balance at both study sites.

site	location	NEE [t C ha^{-1}]	N_2O [kg N ha^{-1}]	CH_4 [kg C ha^{-1}]	harvest [t C ha^{-1}]	fertilizer and seeds [t C ha^{-1}]	NECB [t C ha^{-1}]	GHG balance [t CO_2–eq. ha^{-1}]
REF	field	4.50 ± 1.73			3.17 ± 0.17	1.59	6.08 ± 1.74	26.93 ± 6.57
	between drains		6.37 ± 2.85	−0.48 ± 0.22				
	on a drain pipe		1.42 ± 1.30	1.98 ± 1.55				
INT	field	4.15 ± 1.03			0.57 ± 0.09	0.08	4.64 ± 1.03	77.23 ± 19.31
	between drains		101.35 ± 19.64	0.52 ± 0.94				
	on a drain pipe		187.70 ± 41.00	1.80 ± 1.77				

depths and probably also nutrient availability remained heterogeneous across the field.

3.2.3. *Flux patterns of CO_2 at INT – increasing impact of subsurface irrigation*

Only after a third sowing in August, grass growth finally started and, at least in parts of the field, the young plants had enough water for survival. From September on the increasing impact of raised water levels and first shoots from the last sowing resulted in NEE close to zero at the INT site, whereas at REF net CO_2 emissions were observed (Fig. 3). Comparing also GPP and R_{eco} to the REF site showed that differences in NEE mainly resulted from lower R_{eco} at the INT site. At the end of the balance year, we even saw slightly negative NEE at INT, whereas REF fluxes were still positive. In this phase of the year, this was additionally a result from higher GPP at INT due to the development of the new grass cover probably comprising both above ground and below ground biomass production. However, comparing the partitioned CO_2 fluxes, overall, mostly the establishment of higher water levels and less an increased (aboveground) biomass growth were the main reason for reduced CO_2 emissions at INT compared to REF.

3.2.4. *Net ecosystem carbon balance*

At the REF and INT site, NECB of 6.08 ± 1.74 t C ha^{-1} a^{-1} and 4.64 ± 1.03 t C ha^{-1} a^{-1} were determined, respectively. Methane as well as applied seeds in course of the grassland renewal only marginally contributed to NECB (Table 4). The REF carbon emissions are almost twice as high as the reported mean 3.8 t C ha^{-1} a^{-1} for German grassland on bog peat by Tiemeyer et al. (2016). However, all but one bog peat site in that synthesis study were partially rewetted grassland managed for nature conservation (details in Leiber-Sauheitl et al., 2014 and Förster, 2016). The one intensively managed site (described in detail in Beetz et al., 2013) showed a NECB of 5.4 ± 2.2 t C ha^{-1} a^{-1} (Tiemeyer et al., 2020), which is still slightly lower than the values measured here. Our carbon balance was also higher than the standard emission factor for grasslands on nutrient poor temperate peatlands (5.3 t C ha^{-1} a^{-1}, IPCC, 2014), which is also mainly based on data from less intensively used grasslands. However, the difference is not entirely unambiguous, as this standard emission factor is still within the range of uncertainty of our NECB.

We did not account for losses of dissolved organic carbon (DOC) or other fluvial C losses in this study. However, these fluxes might substantially increase the total C losses: The standard IPCC emission factor for CO_2 emissions from DOC is 0.31 t C ha^{-1} a^{-1} (IPCC, 2014), while Frank (2016) determined losses of 0.32 t C ha^{-1} a^{-1} from an intensively used grassland similar to our REF site. This would correspond to 5% of the NECB determined for the REF site so far. While this is not a large share, losses of DOC from grassland sites with either grassland renewal or subsurface drainage are so far unknown and might require further attention.

Since the publication of the above-mentioned synthesis studies, some more recent literature data on intensively used grassland on bog peat in Denmark and the Netherlands has become available. Compared to these field studies with similar management, our observed emissions were low. The authors determined 11.3 and 13.6 t C ha^{-1} a^{-1} with mean annual water levels of −0.53 and −0.61 m respectively (Weideveld et al., 2021, site B (conventional grazing without mineral soil cover, conventionally drained)) and 10.4 t C ha^{-1} a^{-1} with a mean yearly water level of −0.61 m (Elsgaard et al., 2012) using chamber measurements. Possibly, microbial activity was restrained by the low soil moisture in the topsoil at our REF site explaining the lower net carbon emissions compared to the Danish and Dutch sites (Fig. 4, Fig. 5). This interpretation is supported by incubation studies where highest heterotrophic

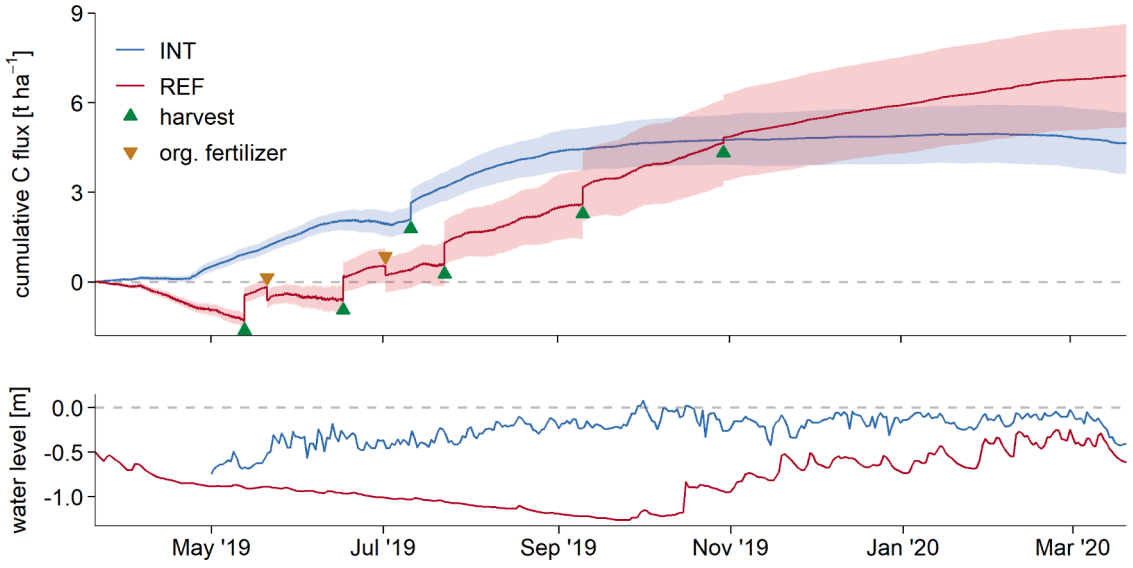

Fig. 4. Top: Cumulative carbon flux including net ecosystem exchange, carbon in harvested biomass, and carbon in applied organic (org.) fertilizer at the REF and INT site. Uncertainty of carbon in harvested material and organic fertilizer is not included in error bands. Bottom: Mean daily water levels at the REF and INT site.

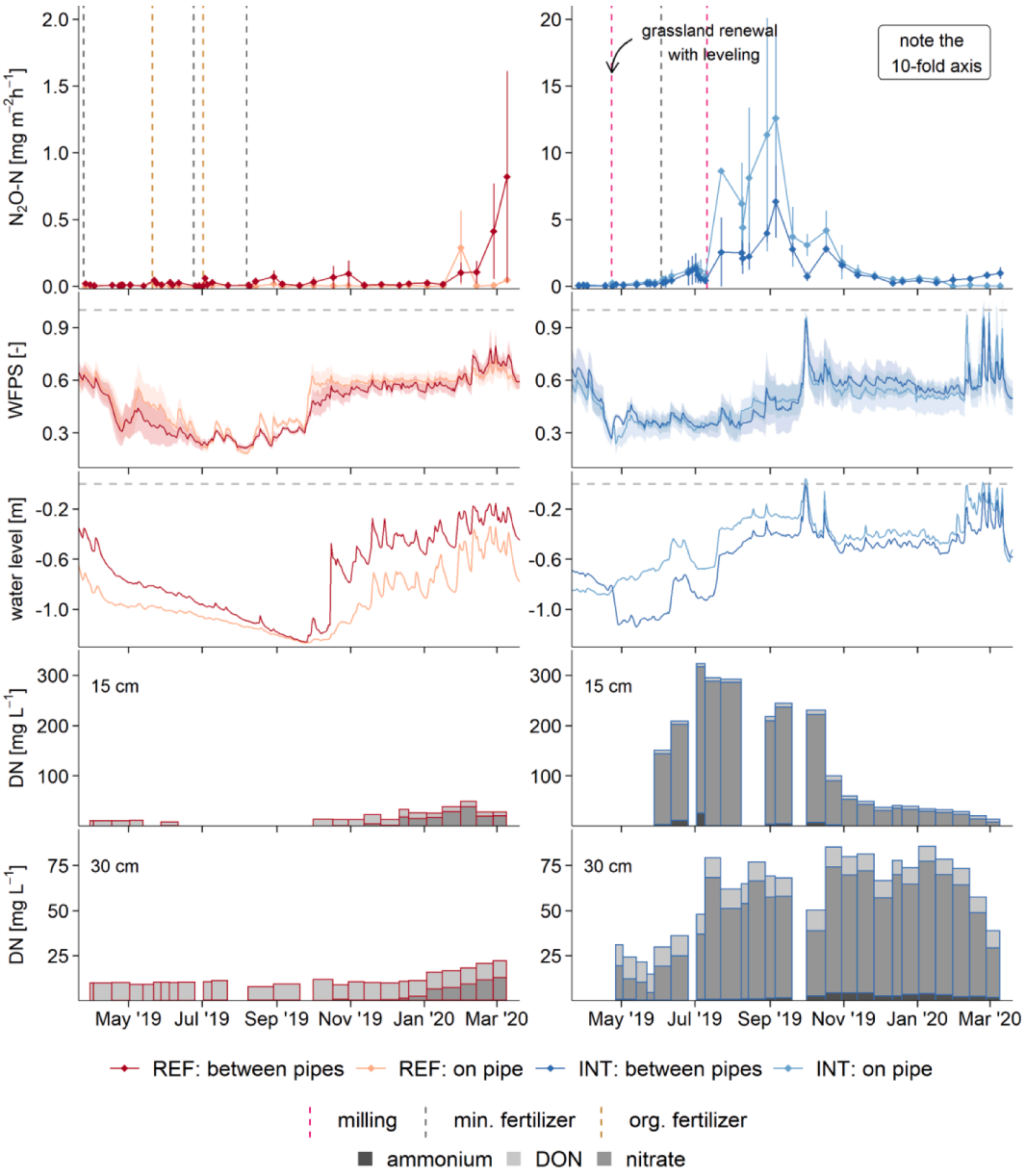

Fig. 5. Nitrous oxide (N_2O) emissions, water filled pore space (WFPS) in 0–5 cm depth, water level, and dissolved nitrogen (DN) in soil water (15 and 30 cm depth) at the REF and INT site.

respiration rates occurred at intermediate soil moisture corresponding to water levels between −0.2 and −0.6 m (Kechavarzi et al., 2010; Säurich et al., 2019). Another possible explanation might be the methodical difference as Weideveld et al. (2021) as well as Elsgaard et al. (2012) used chamber measurements in contrast to the EC technique in this study. This interpretation is supported by estimating NECB (without CH_4) for REF from the mean annual water table depth with equation 2 from Evans et al. (2021) which describes a linear relationship between NECB (without CH_4) and water table depth using a large dataset of only EC measurements. This results in 5.9 t C ha^{-1} a^{-1}, which is very close to our results. However, Beetz et al. (2013) also used chambers and came up with a lower NECB than meausured at our site. Therefore, methodological differences cannot be the only reason for the contrasting results.

The emissions from the INT site are not comparable with other grassland sites on peat due to the renewal measures and no other CO_2 measurements including grassland renewals on peat are published so far. Certainly, the relation of NEE to harvested biomass is extremely unfavorable for this measurement year, as almost no grass could be harvested.

3.3. *Nitrous oxide (N_2O)*

Nitrous oxide emissions were on a very similar, low level prior to the grassland renewal on both sites. Fluxes of almost all campaigns at the REF site were below 0.02 mg N_2O–N m^{-2} h^{-1}. Nitrate concentrations in soil water were low at that time presumably due to uptake by growing biomass as a preceding fertilization prevented any nutrient limitation. At the INT site five out of six fluxes between two drain pipes were not larger than 0.04 mg N_2O–N m^{-2} h^{-1}. Only for fluxes on a drain pipe at INT we saw slightly increased emissions, which however were mostly below 0.1 mg N_2O–N m^{-2} h^{-1} with one exception (0.25 mg N_2O–N m^{-2} h^{-1}). This can probably be explained with the disturbance due to the installation of the drain pipe by cutting approximately 1 m deep into the peat.

3.3.1. Pattern of N_2O fluxes at REF

Nitrous oxide fluxes and balances strongly differed between the two investigated sites. At the REF site the mean flux of all measurement campaigns was 0.03 mg N_2O–N m^{-2} h^{-1}, whereby fluxes only increased markedly in February/March 2020 (flux at 09.03.2020: 0.43 mg N_2O–N m^{-2} h^{-1}). We could not detect any direct reaction to fertilization, in contrast to findings by other studies (Nykänen et al., 1995; Wang et al., 2022). We assume that conditions were too dry for high denitrification rates when fertilization took place. This could for example explain the difference to the study of Wang et al. (2022), who showed increased N_2O emissions after each fertilization from a site in Switzerland during WFPS around 50–80% at 5 cm depth. Except for the first fertilization, we had only 20–40% WFPS in 0–5 cm depth, when fertilization took place. Further, at the REF site increased N_2O emissions occurred at plots between two drain pipes where highest water levels and WFPS occurred in the beginning of 2020 (highest water level: −0.16 m; highest WFPS: 79% in 0-5 cm; Fig. 5). This fits well to findings of incubation experiments of Säurich et al. (2019) where highest N_2O emissions were found for WFPS > 80%, of Wen et al. (2021) who measured highest, intermediate and lowest N_2O emissions at water levels of −0.3, −0.5 and −0.1 m respectively and to a lysimeter experiment of Berglund and Berglund (2011) who found higher N_2O emissions for water levels at −0.4 than at −0.8 m depth. Water filled pore space in the upper soil fluctuated with precipitation, which might additionally contribute to increasing N_2O emissions (Harris et al., 2021; Smith et al., 1998). Simultaneously to higher WFPS from November onwards, nitrate concentrations in sampled soil water increased. As nitrate acts as electron acceptor during denitrification, several studies (Liimatainen et al., 2018; Nykänen et al., 1995) also found higher nitrate concentration corresponding to increased N_2O emissions. Overall, nitrate concentrations (median 0.84 (15 cm depth), 0.15 (30 cm depth) and 0.03 mg N L^{-1} (60 cm depths; not shown)) were typical for intensively used bog peat when compared to findings of Frank et al., 2014 which is higher than in near natural peatlands, but not strongly elevated (Frank et al., 2014).

3.3.2. Pattern of N_2O fluxes at INT – combined impacts of grassland renewal and subsurface irrigation

At our INT site, we measured extremely high N_2O fluxes of up to 12.58 mg N_2O–N m^{-2} h^{-1} after the grassland renewal measures, but only after water levels had been increased by subsurface irrigation. These high emissions could be explained by a combination of drivers: The grassland renewal, the limited grass growth despite a fertilization event, the increased water levels and thus soil moisture and the low pH-value of the peat. All these aspects will be discussed in the following.

Grassland renewal destroyed the old sward and thus enabled the mineralization of the fast decaying young grass litter in addition to the peat organic matter. As R_{eco} stays at a similar level, but GPP drops down significantly, accumulation of nutrients is probable (Fig. 3). This will also have led to N mineralization, as demonstrated by much higher pore water nitrate concentrations prior to fertilization (median 10.70 mg N L^{-1} at 30 cm) than at the REF site (median 0.06 mg N L^{-1} at same depth on the same sampling days). Buchen et al. (2017) found increased emissions rates of up to 6.7 mg N_2O–N m^{-2} h^{-1}, which is only half as high as our maximum value on a drainage pipe, but similar to the highest emissions at the plots between two drain pipes (6.33 mg N_2O–N m^{-2} h^{-1}). However, we did not only measure one distinct peak as Buchen et al. (2017), but sustained high emissions from August 2019 onwards. Ammann et al. (2020) though, found a generally lengthy effect of a grassland renewal on a mineral soil site with increased N_2O emissions during the following two years.

While we did not see significantly increased fluxes directly after the first grassland renewal measures in April, high fluxes have been determined after the repeated measures in July after a preceded mineral fertilization. In accordance to peak N_2O emissions, highest nitrate concentrations appeared in 15 cm depth (highest concentration: 292 mg N L^{-1}), which obviously is one of the key prerequisites for increased N_2O emissions, since nitrate is required for denitrification. Dependencies were found in many other peatland studies (Buchen et al., 2017; Liimatainen et al., 2018; Nykänen et al., 1995) as well as for our REF site, though on a much lower level. In 30 cm depth nitrate concentrations were for a very long time showing a median of 62 mg N L^{-1} between end of July and February. Concentrations in 60 cm stayed low (median: 0.12 mg N L^{-1}; data not shown), thus the risk of losing nitrate through drain water seemed to be low. Still, the median of nitrate concentrations in pore water were alarmingly high and exceeded the EU drinking water limit 26 times at 15 cm and 6 times at 30 cm (Directive (EU) 2020/2184). While nitrate concentrations in drained bogs tend to be relatively low (Frank et al., 2014), concentrations exceeding the drinking water limit have been measured in the discharge of drained fen peat (Tiemeyer and Kahle, 2014). There is little data on the effects of grassland renewal at field scale so far. In a rare study on this topic, Roberts et al. (1986) found that nitrate losses were increased by around 70% even three years after an upland pasture on peat had been ploughed and reseeded. However, as grassland renewal is regularly practiced and not always immediately successful, strongly elevated nitrate concentrations as in our study might not be an isolated case.

Especially at the position of the frames for chamber measurements, grass growth was extremely poor and germination struggled until the end of the study. Therefore, nitrate and other nutrients in the pore water could not be reduced by biomass uptake and plants did not compete with microorganisms for the consumption of nutrients. Nitrous oxide emissions have been found to positively correlate with nutrient availability (P, K) in other studies (Liimatainen et al., 2018; Mehnaz and Dijkstra, 2016; Säurich et al., 2019) which could be important in our case, too. Further, findings of Merbold et al. (2014) on a mineral soil site, showed that plant activity is an influencing factor for N_2O emissions. In detail, availability of nitrogen may lead to higher CO_2 uptake through photosynthesis or if plant activity is low it may lead to higher N_2O emissions through denitrification. Buchen et al. (2017) also found a relation between microbial activity, visible for example in CO_2 emissions, which originates from heterotrophic respiration in our case when plants were absent in measurement frames, and N_2O fluxes. At our site, nitrate concentration in 15 cm depth increased until July and stayed at an extremely high level until October, when concurrently N_2O emissions dropped down. By this time, most of the nitrate had probably been denitrified or leached, as the nitrate concentrations were still slightly rising until the maximum was reached in autumn in 30 cm depths. However, high concentrations were not found in deeper (60 cm) layers.

Besides rising nitrate concentrations, WFPS was increasing from August onwards, establishing even more favorable conditions for denitrification. Water filled pore space plays a key role for N_2O emissions in peatlands (Berglund and Berglund, 2011; Buchen et al., 2017; Säurich et al., 2019; Wen et al., 2021). At the plots on a drain pipe with higher water levels, maximum emissions were twice as high as between two drain pipes, however WFPS was similar in 0–5 cm depth. Comparing water levels measured at the plots, it is most likely that WFPS below 5 cm was higher on a drain pipe than between two drain pipes. Water levels were in fact 15 to 20 cm higher on a drain pipe than between two drain pipes, when peak emissions occurred. Although on a different magnitude, these results are comparable to Wen et al. (2021) and Berglund and Berglund (2011), who found higher emissions with water levels at −0.3 m than at −0.5 m and at −0.4 m than at −0.8 m, respectively. While in our case, the subsurface irrigation caused the increase in water level and soil moisture, a similarly adverse situation could probably occur due to prolonged rainfall.

One additional reason for our high N_2O emissions might also be the typically low pH (3.7–4.4) of bog peat in the upper horizon. Low pH values are reported to inhibit the last step of denitrification from N_2O to N_2 (Bakken et al., 2012). The relevance of the pH value could be shown in some peatland studies (Flessa et al., 1998; Regina et al., 1996; Weslien et al., 2009), while there was no effect in others (Liimatainen et al., 2018; Maljanen et al., 2010). This is not surprising, as for high N_2O

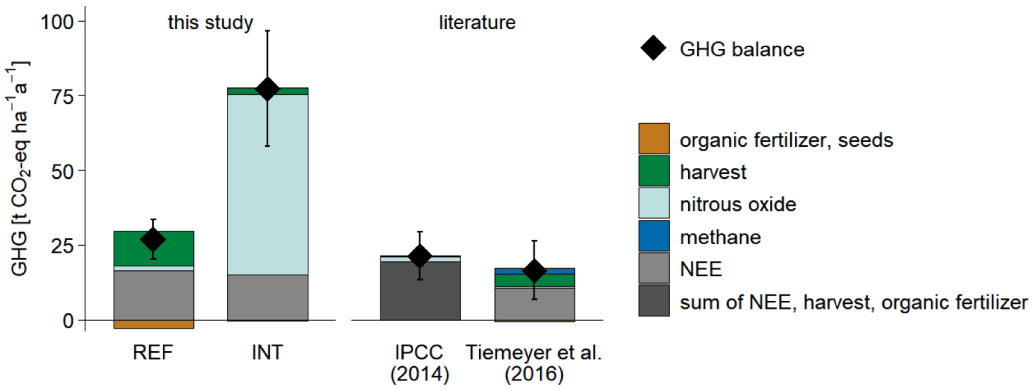

Fig. 6. Greenhouse gas (GHG) balance and their components net ecosystem exchange (NEE), methane, nitrous oxide, carbon export in harvested biomass and carbon input from organic fertilizer and seeds are shown for the REF and INT site and for data from Tiemeyer et al. (2016) for German grassland on bog peat as well as IPCC default values for grassland on nutrient-poor peat (IPCC, 2014). In case of IPCC (2014), CO_2-eq. of NEE, organic fertilizer, and harvest are not separately available.

emissions, the fulfillment of one prerequisite (e.g. pH value, high nitrate availability) is usually not sufficient. In the case of the INT site, all relevant prerequisites for high N_2O emissions (via denitrification) coincide and thus result in unprecedented high fluxes.

3.3.3. *Annual N_2O emissions*

With 3.9 ± 3.1 kg N_2O–N ha^{-1} a^{-1} the annual N_2O emissions at the REF site are well in line with IPCC standard emission factors for grassland on drained, nutrient poor temperate peatlands (4.3 kg N_2O–N ha^{-1} a^{-1}; IPCC, 2014) but higher than emissions from German grasslands on bog peat (Tiemeyer et al., 2016) with 1.8 kg N_2O–N ha^{-1} a^{-1}. As already described, data from this study originates mainly from grasslands with low intensity use and thus lower or no N fertilization. However, N_2O fluxes were smaller than in Buchen et al. (2017; 6.26 ± 3.10 and 6.54 ± 3.92 kg N_2O–N ha^{-1} a^{-1}) but with regard to uncertainties comparable.

At the INT site, we calculated total annual N_2O emissions of 144.5 ± 45.5 kg N_2O–N ha^{-1} a^{-1}, which is to our best knowledge the highest ever reported annual N_2O emission from organic soils. Highest emissions so far (56.4 kg N_2O–N ha^{-1} a^{-1}) were found for an unfertilized arable field (Flessa et al., 1998). For organic soils, the only publication on grassland renewal found a significant increase of N_2O fluxes for two month, but no effect on annual budgets, which are, even in the one year with highest fluxes, more than one magnitude lower than our results (9.88 ± 4.55 kg N_2O–N ha^{-1} a^{-1}, year 2013/2014; Buchen et al., 2017). However, they did not report any problems with the renewal procedures as in our case. Still, looking at other grassland sites in northern Germany conducting renewals in the same year 2019 with low precipitation in spring, germinating was often not more successful than at our INT site.

3.4. *Greenhouse gas balance*

For the REF site, we calculated a total GHG balance of 26.9 ± 6.6 t CO_2–eq. ha^{-1} a^{-1}, with the two largest components being NEE and harvest. As both CO_2 and N_2O emissions were higher than those reported for German grassland on bog peat (Tiemeyer et al., 2016), our total GHG emissions were larger than the average for bog peat, too (Fig. 6). Only when comparing to all included German peatland sites in this study the total GHG balance is similar, which would include fen peat with a higher nutrient status and all other organic soils. Our total GHG emissions at REF are still around 4 t CO_2–eq. ha^{-1} a^{-1}higher than the average from the intensively managed grassland site in Beetz et al. (2013) and also higher than the IPCC (2014) default value for grassland on nutrient-poor peat (21.3 t CO_2–eq. ha^{-1} a^{-1}), but within the range of uncertainties.

At the INT site, the extremely high N_2O emissions, caused by the grassland renewal and the related combination of circumstances including raised water levels, clearly dominated the total GHG balance. Thus, total emissions of 77.2 ± 19.3 t CO_2–eq. ha^{-1} a^{-1} were very high as well. To our best knowledge there are no other studies on annual GHG emissions comprising CO_2, CH_4, and N_2O measurements including grassland renewal measures to which we could compare our results.

4. Conclusions

Greenhouse gas emissions of deeply drained bog peat under intensive grassland use (REF site) were higher than most values previously reported for grassland on nutrient-poor peat, probably due to the lower land use intensity of sites studied so far. At the second studied site (INT) with a SI system, a combination of mechanical grassland renewal, including leveling, poor grass growth and raised water levels by subsurface irrigation resulted in a strong increase of GHG emissions in the first year after implementation. Particularly, we measured the highest ever published N_2O emissions from organic soils at our INT site caused by an interaction of high nitrate availability due to mineralization induced by (repeated) renewal measures, poor grass growth and fertilization on the one hand and moist conditions favoring denitrification on the other hand, possibly enhanced by the low pH of the peat. Net ecosystem carbon balance was lower at the INT site than at the REF site, although with high efforts of repeated grassland renewal measures and only marginal harvest.

When transformed into CO_2-equivalents, N_2O emissions consequently dominated the GHG balance at INT, which exceeded all values measured for drained bog peat so far. However, there are no studies on the effect of grassland renewal on all GHGs for organic soils available in literature so far.

This is only one first year of GHG data where the effects of the mechanical grassland renewal dominated the reaction of the ecosystem. During the later stage of the study, net ecosystem exchange decreased with higher water levels, which gives hope for a reduction of CO_2 emissions in the upcoming years. Certainly, a longer monitoring period will be required to ascertain the overall effects of SI. However, as SI is meant to act as a climate mitigation measure, the installation of such a system should be conducted with care to avoid a negative climate effect in the beginning.

As leveling did not improve the applicability of subsurface irrigation as shown by the still spatially heterogeneous water levels, the entire grassland renewal seems to have been rather pointless regarding harvest failure of almost an entire year as well as the unnecessarily high GHG emissions. The results of this study show that mechanical grassland renewals on organic soils should be avoided and a careful maintenance of grassland sites is very important to omit renewals more often than in the past. A coincidence of grassland renewal measures with sparse grass growth and wet conditions is not necessarily a result of subsurface irrigation, but could also be caused by prolonged rainfall. Still, special attention should be payed when grassland renewal and water level

management is practiced at the same time to prevent N_2O emission peaks.

Declaration of Competing Interest

The authors declare that they have no known competing financial interests or personal relationships that could have appeared to influence the work reported in this paper.

Data Availability

Data will be made available on request.

Acknowledgements

The project "Gnarrenburger Moor" (application no. ZW 6–85023359) is funded by the European Regional Development Fund, the Lower Saxony Ministry of Food, Agriculture and Consumer Protection and the Lower Saxony Ministry of the Environment, Energy and Climate Protection.

Chris Evans and an anonymous reviewer greatly helped to improve the manuscript by insightful comments and suggestions.

We thank the project team of the Project “Gnarrenburger Moor” at the State Authority for Mining, Energy and Geology Lower Saxony and at the Chamber of Agriculture. Special thanks also to the cooperating farmers.

We also want to express our thanks to Arne Heidkamp and Daniel Ziehe with their laboratory teams, especially Kerstin Gilke and Andrea Oehns-Rittgerodt for gas chromatograph analyses. Andrea Niemeyer, Manuela Rutsch, Adina Schlegel, Nicole Altwein, Ute Tambor, Sabine Wathsack, Dagmar Wenderoth, and Claudia Wiese for water, soil, and biomass analyses.

Thanks also to the State Authority for Mining, Energy and Geology Lower Saxony for provision of water level and surface elevation data.

We further thank Jean-Pierre Delorme, Jens-Kristian Jüdt, Frank Hegewald, Dirk Lempio, and Thomas Viohl for technical assistance in the field.

We also want to thank all members of the working groups of Bärbel Tiemeyer and Christian Brümmer at the Thünen Institute of Climate-Smart Agriculture for all kinds of help in the field, as well as for technical and scientific support.

Finally, we would like to thank all the students who helped in the field and in the laboratory, especially Marit Baumeister and Timothy Husting.

References

Ad-Hoc-AG Boden (Ad Hoc Arbeitsgruppe Boden), 2005. Bodenkundliche Kartieranleitung KA5 (Manual of Soil Mapping), 5th ed. Schweizerbart’sche Verlagsbuchhandlung, Hanover, Germany.

Ammann, C., Neftel, A., Jocher, M., Fuhrer, J., Leifeld, J., 2020. Effect of management and weather variations on the greenhouse gas budget of two grasslands during a 10-year experiment. Agric. Ecosyst. Environ. 292, 106814 https://doi.org/10.1016/j.agee.2019.106814.

Aubinet, M., Grelle, A., Ibrom, A., Rannik, Ü., Moncrieff, J.B., Foken, T., Kowalski, A.S., Martin, P.H., Berbigier, P., Bernhofer, C., Clement, R., Elbers, J., Granier, A., Grünwald, T., Morgenstern, K., Pilegaard, K., Rebmann, C., Snijders, W., Valentini, R., Vesala, T., 1999. Estimates of the annual net carbon and water exchange of forests: the EUROFLUX methodology. Adv. Ecol. Res. 30, 113–175. https://doi.org/10.1016/S0065-2504(08)60018-5.

Bader, C., Müller, M., Schulin, R., Leifeld, J., 2017. Amount and stability of recent and aged plant residues in degrading peatland soils. Soil Biol. Biochem. 109, 167–175. https://doi.org/10.1016/j.soilbio.2017.01.029.

Bakken, L.R., Bergaust, L., Liu, B., Frostegård, A., 2012. Regulation of denitrification at the cellular level: a clue to the understanding of N_2O emissions from soils. Philos. Trans. R. Soc. London, Ser. B 367 (1593), 1226–1234. https://doi.org/10.1098/rstb.2011.0321.

Beetz, S., Liebersbach, H., Glatzel, S., Jurasinski, G., Buczko, U., Höper, H., 2013. Effects of land use intensity on the full greenhouse gas balance in an Atlantic peat bog. Biogeosciences 10 (2), 1067–1082. https://doi.org/10.5194/bg-10-1067-2013.

Berglund, Ö., Berglund, K., 2011. Influence of water table level and soil properties on emissions of greenhouse gases from cultivated peat soil. Soil Biol. Biochem. 43 (5), 923–931. https://doi.org/10.1016/j.soilbio.2011.01.002.

Boonman, J., Hefting, M.M., van Huissteden, C.J.A., van den Berg, M., van Huissteden, J., Erkens, G., Melman, R., van der Velde, Y., 2021. Cutting peatland CO_2 emissions with rewetting measures. Biogeosciences Discuss 1–31. https://doi.org/10.5194/bg-2021-276 [preprint].

Buchen, C., Well, R., Helfrich, M., Fuß, R., Kayser, M., Gensior, A., Benke, M., Flessa, H., 2017. Soil mineral N dynamics and N_2O emissions following grassland renewal. Agric. Ecosyst. Environ. 246, 325–342. https://doi.org/10.1016/j.agee.2017.06.013.

Butterbach-Bahl, K., Baggs, E.M., Dannenmann, M., Kiese, R., Zechmeister-Boltenstern, S., 2013. Nitrous oxide emissions from soils: how well do we understand the processes and their controls? Philos. Trans. R. Soc. London, Ser. B 368 (1621), 20130122. https://doi.org/10.1098/rstb.2013.0122.

D’Angelo, B., Gogo, S., Laggoun-Défarge, F., Le Moing, F., Jégou, F., Guimbaud, C., 2016. Soil temperature synchronisation improves representation of diel variability of ecosystem respiration in *Sphagnum* peatlands. Agric. For. Meteorol. 223, 95–102. https://doi.org/10.1016/j.agrformet.2016.03.021.

den Hartogh, J.H., 2014. The impact of submerged drainage on groundwater level, soil subsidence, bearing capacity, and grass production. Master thesis. Wageningen University.

DIN EN ISO 11885:2009-09, 2009. Water quality - determination of selected elements by inductively coupled plasma optical emission spectrometry (ICP-OES). Beuth Verlag GmbH, Berlin, Germany. https://doi.org/10.31030/1530145.

DIN ISO 10390:2005-12, 2005. Soil quality - determination of pH. Beuth Verlag GmbH, Berlin, Germany.

Directive (EU) 2020/2184 of the European parliament and of the council of 16 December 2020 on the quality of water intended for human consumption.

Durner, W., 1994. Hydraulic conductivity estimation for soils with heterogeneous pore structure. Water Resour. Res. 30 (2), 211–223. https://doi.org/10.1029/93wr02676.

Elsgaard, L., Görres, C.-.M., Hoffmann, C.C., Blicher-Mathiesen, G., Schelde, K., Petersen, S.O., 2012. Net ecosystem exchange of CO_2 and carbon balance for eight temperate organic soils under agricultural management. Agric. Ecosyst. Environ. 162, 52–67. https://doi.org/10.1016/j.agee.2012.09.001.

Evans, C.D., Peacock, M., Baird, A.J., Artz, R.R.E., Burden, A., Callaghan, N., Chapman, P.J., Cooper, H.M., Coyle, M., Craig, E., Cumming, A., Dixon, S., Gauci, V., Grayson, R.P., Helfter, C., Heppell, C.M., Holden, J., Jones, D.L., Kaduk, J., Levy, P., Matthews, R., McNamara, N.P., Misselbrook, T., Oakley, S., Page, S.E., Rayment, M., Ridley, L.M., Stanley, K.M., Williamson, J.L., Worrall, F., Morrison, R., 2021. Overriding water table control on managed peatland greenhouse gas emissions. Nature 593, 548–552. https://doi.org/10.1038/s41586-021-03523-1.

Finkelstein, P.L., Sims, P.F., 2001. Sampling error in eddy correlation flux measurements. J. Geophys. Res. D: Atmos. 106 (D4), 3503–3509. https://doi.org/10.1029/2000JD900731.

Firestone, M.K., Davidson, E.A., 1989. Microbiological basis of NO and N_2O production and consumption in soil. Exchange of trace gases between terrestrial ecosystems and the atmosphere 47, 7–21.

Flessa, H., Wild, U., Klemisch, M., Pfadenhauer, J., 1998. Nitrous oxide and methane fluxes from organic soils under agriculture. Eur. J. Soil. Sci. 49, 327–335. https://doi.org/10.1046/j.1365-2389.1998.00156.x.

Förster, C., 2016. Influence of management and restoration on greenhouse gas fluxes of a prealpine bog. Dissertation, Munich, 143 pp.

Frank, S., Tiemeyer, B., Gelbrecht, J., Freibauer, A., 2014. High soil solution carbon and nitrogen concentrations in a drained Atlantic bog are reduced to natural levels by 10 years of rewetting. Biogeosciences 11 (8), 2309–2324. https://doi.org/10.5194/bg-11-2309-2014.

Frolking, S., Roulet, N., 2007. Holocene radiative forcing impact of northern peatland carbon accumulation and methane emissions. Global Change Biol 13, 1079–1088. https://doi.org/10.1111/j.1365-2486.2007.01339.x.

Frolking, S., Roulet, N., Fuglestvedt, J., 2006. How northern peatlands influence the Earth’s radiative budget: sustained methane emission versus sustained carbon sequestration. J. Geophys. Res. G: Biogeosci. 111 (G01008) https://doi.org/10.1029/2005JG000091.

Fu, Z., Ciais, P., Makowski, D., Bastos, A., Stoy, P.C., Ibrom, A., Knohl, A., Migliavacca, M., Cuntz, M., Šigut, L., Peichl, M., Loustau, D., El-Madany, T.S., Buchmann, N., Gharun, M., Janssens, I., Markwitz, C., Grünwald, T., Rebmann, C., Mölder, M., Varlagin, A., Mammarella, I., Kolari, P., Bernhofer, C., Heliasz, M., Vincke, C., Pitacco, A., Cremonese, E., Foltýnová, L., Wigneron, J.-.P., 2022. Uncovering the critical soil moisture thresholds of plant water stress for European ecosystems. Global Change Biol 28 (6), 2111–2123. https://doi.org/10.1111/gcb.16050.

Fuß, R., 2020. gasfluxes: greenhouse gas flux calculation from chamber measurements (v. 0.4-4).

Gash, J.H.C., Culf, A.D., 1996. Applying a linear detrend to eddy correlation data in realtime. Boundary-Layer Meteorol 79, 301–306. https://doi.org/10.1007/BF00119443.

Graeber, D., Gelbrecht, J., Kronvang, B., Gücker, B., Pusch, M.T., Zwirnmann, E., 2012. Technical note: Comparison between a direct and the standard, indirect method for dissolved organic nitrogen determination in freshwater environments with high dissolved inorganic nitrogen concentrations. Biogeosciences 9 (11), 4873–4884. https://doi.org/10.5194/bg-9-4873-2012.

Günther, A., Huth, V., Jurasinski, G., Glatzel, S., 2015. The effect of biomass harvesting on greenhouse gas emissions from a rewetted temperate fen. GCB Bioenergy 7 (5), 1092–1106. https://doi.org/10.1111/gcbb.12214.

Harris, C.I., Erickson, T.H., Ellis, N.K., Larson, J.E., 1962. Water-level control in organic soil, as related to subsidence rate, crop yield, and response to nitrogen. Soil Sci 94 (3), 158–161.

Harris, E., Diaz-Pines, E., Stoll, E., Schloter, M., Schulz, S., Duffner, C., Li, K., Moore, K.L., Ingrisch, J., Reinthaler, D., Zechmeister-Boltenstern, S., Glatzel, S., Brüggemann, N., Bahn, M., 2021. Denitrifying pathways dominate nitrous oxide emissions from managed grassland during drought and rewetting. Sci Adv 7 (6), eabb7118. https://doi.org/10.1126/sciadv.abb7118.

Hüppi, R., Feilber, R., Krauss, M., Six, J., Leifeld, J., Fuß, R., 2018. Restricting the nonlinearity parameter in soil greenhouse gas flux calculation for more reliable flux estimates. PLoS ONE 13 (7), e0200876. https://doi.org/10.5281/ZENODO.1310924.

IPCC (Intergovernmental Panel on Climate Change), 2014. In: 2013 Supplement to the 2006 IPCC Guidelines for National Greenhouse Gas Inventories: Wetlands. IPCC, Switzerland.

IUSS Working Group WRB, 2015. World reference base for soil resources 2014, update 2015: international soil classification system for naming soils and creating legends for soil maps. World Soil Resources Reports No. 106. FAO, Rome.

Juszczak, R., Humphreys, E., Acosta, M., Michalak-Galczewska, M., Kayzer, D., Olejnik, J., 2013. Ecosystem respiration in a heterogeneous temperate peatland and its sensitivity to peat temperature and water table depth. Plant Soil 366 (1–2), 505–520. https://doi.org/10.1007/s11104-012-1441-y.

Kayser, M., Müller, J., Isselstein, J., 2018. Grassland renovation has important consequences for C and N cycling and losses. Food Energy Secur 7 (4), e00146. https://doi.org/10.1002/fes3.146.

Kechavarzi, C., Dawson, Q., Bartlett, M., Leeds-Harrison, P.B., 2010. The role of soil moisture, temperature and nutrient amendment on CO_2 efflux from agricultural peat soil microcosms. Geoderma 154 (3–4), 203–210. https://doi.org/10.1016/j.geoderma.2009.02.018.

Kljun, N., Calanca, P., Rotach, M.W., Schmid, H.P., 2015. A simple two-dimensional parameterisation for flux footprint prediction (FFP). Geosci. Model Dev. 8 (11), 3695–3713. https://doi.org/10.5194/gmd-8-3695-2015.

Kljun, N., Rotach, M.W., Schmid, H.P., 2002. A three-dimensional backward lagrangian footprint model for a wide range of boundary-layer stratifications. Boundary-Layer Meteorol. 103, 205–226. https://doi.org/10.1023/A:1014556300021.

Komulainen, V.-M., Tuittila, E.-S., Vasander, H., Laine, J., 1999. Restoration of drained peatlands in southern Finland: initial effects on vegetation change and CO_2 balance. J. Appl. Ecol. 36, 634–648. https://doi.org/10.1046/j.1365-2664.1999.00430.x.

Krol, D.J., Jones, M.B., Williams, M., Richards, K.G., Bourdin, F., Lanigan, G.J., 2016. The effect of renovation of long-term temperate grassland on N_2O emissions and N leaching from contrasting soils. Sci. Total Environ. 560-561, 233–240. https://doi.org/10.1016/j.scitotenv.2016.04.052.

Lafleur, P.M., Moore, T.R., Roulet, N.T., Frolking, S., 2005. Ecosystem respiration in a cool temperate bog depends on peat temperature but not water table. Ecosystems 8 (6), 619–629. https://doi.org/10.1007/s10021-003-0131-2.

Larmola, T., Bubier, J.L., Kobyljanec, C., Basiliko, N., Juutinen, S., Humphreys, E., Preston, M., Moore, T.R., 2013. Vegetation feedbacks of nutrient addition lead to a weaker carbon sink in an ombrotrophic bog. Global Change Biol 19 (12), 3729–3739. https://doi.org/10.1111/gcb.12328.

Leiber-Sauheitl, K., Fuß, R., Voigt, C., Freibauer, A., 2014. High CO_2 fluxes from grassland on histic Gleysol along soil carbon and drainage gradients. Biogeosciences 11 (3), 749–761. https://doi.org/10.5194/bg-11-749-2014.

Leppelt, T., Dechow, R., Gebbert, S., Freibauer, A., Lohila, A., Augustin, J., Drösler, M., Fiedler, S., Glatzel, S., Höper, H., Järveoja, J., Lærke, P.E., Maljanen, M., Mander, Ü., Mäkiranta, P., Minkkinen, K., Ojanen, P., Regina, K., Strömgren, M., 2014. Nitrous oxide emission budgets and land-use-driven hotspots for organic soils in Europe. Biogeosciences 11 (23), 6595–6612. https://doi.org/10.5194/bg-11-6595-2014.

LI-COR, 2022. EddyPro® Software, Help function, online source, last access: 05.06.2022.

Liimatainen, M., Voigt, C., Martikainen, P.J., Hytönen, J., Regina, K., Óskarsson, H., Maljanen, M., 2018. Factors controlling nitrous oxide emissions from managed northern peat soils with low carbon to nitrogen ratio. Soil Biol. Biochem. 122, 186–195. https://doi.org/10.1016/j.soilbio.2018.04.006.

Loisel, J., Yu, Z., Beilman, D.W., Camill, P., Alm, J., Amesbury, M.J., Anderson, D., Andersson, S., Bochicchio, C., Barber, K., Belyea, L.R., Bunbury, J., Chambers, F.M., Charman, D.J., Vleeschouwer, F.de, Fiałkiewicz-Kozieł, B., Finkelstein, S.A., Gałka, M., Garneau, M., Hammarlund, D., Hinchcliffe, W., Holmquist, J., Hughes, P., Jones, M.C., Klein, E.S., Kokfelt, U., Korhola, A., Kuhry, P., Lamarre, A., Lamentowicz, M., Large, D., Lavoie, M., MacDonald, G., Magnan, G., Mäkilä, M., Mallon, G., Mathijssen, P., Mauquoy, D., McCarroll, J., Moore, T.R., Nichols, J., O'Reilly, B., Oksanen, P., Packalen, M., Peteet, D., Richard, P.J.H., Robinson, S., Ronkainen, T., Rundgren, M., Sannel, A.B.K., Tarnocai, C., Thom, T., Tuittila, E.-S., Turetsky, M., Väliranta, M., van der Linden, M., van Geel, B., van Bellen, S., Vitt, D., Zhao, Y., Zhou, W., 2014. A database and synthesis of northern peatland soil properties and Holocene carbon and nitrogen accumulation. The Holocene 24 (9), 1028–1042. https://doi.org/10.1177/0959683614538073.

Lucas-Moffat, A.M., Huth, V., Augustin, J., Brümmer, C., Herbst, M., Kutsch, W.L., 2018. Towards pairing plot and field scale measurements in managed ecosystems: using eddy covariance to cross-validate CO_2 fluxes modeled from manual chamber campaigns. Agric. For. Meteorol. 256-257 (3), 362–378. https://doi.org/10.1016/j.agrformet.2018.01.023.

Malicki, M.A., Plagge, R., Roth, C.H., 1996. Improving the calibration of dielectric TDR soil moisture determination taking into account the solid soil. Eur. J. Soil. Sci. 47 (3), 357–366. https://doi.org/10.1111/j.1365-2389.1996.tb01409.x.

Maljanen, M., Sigurdsson, B.D., Guðmundsson, J., Óskarsson, H., Huttunen, J.T., Martikainen, P.J., 2010. Greenhouse gas balances of managed peatlands in the Nordic countries – present knowledge and gaps. Biogeosciences 7 (9), 2711–2738. https://doi.org/10.5194/bg-7-2711-2010.

Mauder, M., Cuntz, M., Drüe, C., Graf, A., Rebmann, C., Schmid, H.P., Schmidt, M., Steinbrecher, R., 2013. A strategy for quality and uncertainty assessment of long-term eddy-covariance measurements. Agric. For. Meteorol. 169, 122–135. https://doi.org/10.1016/j.agrformet.2012.09.006.

Mauder, M., Foken, T., 2004. Documentation and instruction manual of the eddy covariance software package TK2. Universität Bayreuth, Abt. Mikrometeorologie, Bayreuth, p. 45.

Mehnaz, K.R., Dijkstra, F.A., 2016. Denitrification and associated N_2O emissions are limited by phosphorus availability in a grassland soil. Geoderma 284 (3), 34–41. https://doi.org/10.1016/j.geoderma.2016.08.011.

Merbold, L., Eugster, W., Stieger, J., Zahniser, M., Nelson, D., Buchmann, N., 2014. Greenhouse gas budget (CO_2, CH_4 and N_2O) of intensively managed grassland following restoration. Global Change Biol. 20 (6), 1913–1928. https://doi.org/10.1111/gcb.12518.

Moffat, A.M., Papale, D., Reichstein, M., Hollinger, D.Y., Richardson, A.D., Barr, A.G., Beckstein, C., Braswell, B.H., Churkina, G., Desai, A.R., Falge, E., Gove, J.H., Heimann, M., Hui, D., Jarvis, A.J., Kattge, J., Noormets, A., Stauch, V.J., 2007. Comprehensive comparison of gap-filling techniques for eddy covariance net carbon fluxes. Agric. For. Meteorol. 147 (3–4), 209–232. https://doi.org/10.1016/j.agrformet.2007.08.011.

Moncrieff, J., Clement, R., Finnigan, J., Meyers, T., 2004. Averaging, Detrending, and Filtering of Eddy Covariance Time Series. In: Lee, X., Massman, W., Law, B. (Eds.), Handbook of Micrometeorology. Atmospheric and Oceanographic Sciences Library. Springer, Dordrecht. https://doi.org/10.1007/1-4020-2265-4_2 vol 29.

Moncrieff, J.B., Massheder, J.M., Bruin, H.de, Elbers, J., Friborg, T., Heusinkveld, B., Kabat, P., Scott, S., Soegaard, H., Verhoef, A., 1997. A system to measure surface fluxes of momentum, sensible heat, water vapour and carbon dioxide. J Hydrol (Amst) 188-189 (Suppl. II), 589–611. https://doi.org/10.1016/S0022-1694(96)03194-0.

Moore, T.R., Knowles, R., 1989. The influence of water table levels on methane and carbon dioxide emissions from peatland soils. Can. J. Soil Sci. 69, 33–38. https://doi.org/10.4141/cjss89-004.

Mualem, Y., 1976. A new model for predicting the hydraulic conductivity of unsaturated porous media. Water Resour. Res. 12 (3), 513–522. https://doi.org/10.1029/WR012i003p00513.

Myhre, G., Shindell, D., Bréon, F.-M., Collins, W., Fuglestvedt, J., Huang, J., Koch, D., Lamarque, J.-F., Lee, D., Mendoza, B., Nakajima, T., Robock, A., Stephens, G., Takemura, T., Zhang, H., et al., 2013. Anthropogenic and Natural Radiative Forcing. In: Stocker, T.F., Qin, D., Plattner, G.-K., Tignor, M., Allen, S.K., Boschung, J., et al. (Eds.), Climate Change 2013: The Physical Science Basis. Contribution of Working Group I to the Fifth Assessment Report of the Intergovernmental Panel on Climate Change. Cambridge University Press, Cambridge, United Kingdom and New York, NY, USA. https://doi.org/10.1017/CBO9781107415324.018.

Nykänen, H., Alm, J., Lang, K., Silvola, J., Martikainen, P.J., 1995. Emissions of CH_4, N_2O and CO_2 from a virgin fen and a fen drained for grassland in Finland. J. Biogeogr. 22, 351–357. https://doi.org/10.2307/2845930.

Oestmann, J., Tiemeyer, B., Düvel, D., Grobe, A., Dettmann, U., 2022. Greenhouse gas balance of sphagnum farming on highly decomposed peat at former peat extraction sites. Ecosystems 25 (2), 350–371. https://doi.org/10.1007/s10021-021-00659-z.

Op de Beek, M., Sabbatini, S., Papale, D., 2017. ICOS Ecosystem Instructions for Ancillary Vegetation Measurements in Grasslands (Version 2020-03-16). ICOS Ecosystem Thematic Centre. https://doi.org/10.18160/daaa-x1ng.

Papale, D., Reichstein, M., Aubinet, M., Canfora, E., Bernhofer, C., Kutsch, W., Longdoz, B., Rambal, S., Valentini, R., Vesala, T., Yakir, D., 2006. Towards a standardized processing of net ecosystem exchange measured with eddy covariance technique: algorithms and uncertainty estimation. Biogeosciences 3, 571–583. https://doi.org/10.5194/bg-3-571-2006.

Pedersen, A.R., Petersen, S.O., Schelde, K., 2010. A comprehensive approach to soil-atmosphere trace-gas flux estimation with static chambers. Eur. J. Soil Sci. 61 (6), 888–902. https://doi.org/10.1111/j.1365-2389.2010.01291.x.

Priesack, E., Durner, W., 2006. Closed-form expression for the multi-modal unsaturated conductivity function. Vadose Zone J 5 (1), 121–124. https://doi.org/10.2136/vzj2005.0066.

R Core Team, 2020. R: a language and environment for statistical computing. R Foundation for Statistical Computing, Vienna, Austria.

Regina, K., Hykänen, H., Silvola, J., Martkainen, P.J., 1996. Fluxes of nitrous oxide from boreal peatlands as affected by peatland type, water table level and nitrification capacity. Biogeochemistry 35, 401–418. https://doi.org/10.1007/BF02183033.

Reichstein, M., Falge, E., Baldocchi, D., Papale, D., Aubinet, M., Berbigier, P., Bernhofer, C., Buchmann, N., Gilmanov, T., Granier, A., Grunwald, T., Havrankova, K., Ilvesniemi, H., Janous, D., Knohl, A., Laurila, T., Lohila, A., Loustau, D., Matteucci, G., Meyers, T., Miglietta, F., Ourcival, J.-M., Pumpanen, J., Rambal, S., Rotenberg, E., Sanz, M., Tenhunen, J., Seufert, G., Vaccari, F., Vesala, T., Yakir, D., Valentini, R., 2005. On the separation of net ecosystem exchange into assimilation and ecosystem respiration: review and improved algorithm. Global Change Biol 11 (9), 1424–1439. https://doi.org/10.1111/j.1365-2486.2005.001002.x.

Repo, M.E., Susiluoto, S., Lind, S.E., Jokinen, S., Elsakov, V., Biasi, C., Virtanen, T., Martikainen, P.J., 2009. Large N_2O emissions from cryoturbated peat soil in tundra. Nat. Geosci. 2 (3), 189–192. https://doi.org/10.1038/ngeo434.

Richardson, D., Felgate, H., Watmough, N., Thomson, A., Baggs, E., 2009. Mitigating release of the potent greenhouse gas N_2O from the nitrogen cycle - could enzymic regulation hold the key? Trends Biotechnol. 27 (7), 388–397. https://doi.org/10.1016/j.tibtech.2009.03.009.

Roberts, G., Hudson, J.A., Blackie, J.R., 1986. Effects of upland pasture improvement on nutrient release in flows from a "natural" lysimeter and a field drain. Agr. Water Manage. 11, 237–245. https://doi.org/10.1016/0378-3774(86)90041-7.

Rutledge, S., Wall, A.M., Mudge, P.L., Troughton, B., Campbell, D.I., Pronger, J., Joshi, C., Schipper, L.A., 2017. The carbon balance of temperate grasslands part II: the impact of pasture renewal via direct drilling. Agric. Ecosyst. Environ. 239, 132–142. https://doi.org/10.1016/j.agee.2017.01.013.

Säurich, A., Tiemeyer, B., Dettmann, U., Don, A., 2019. How do sand addition, soil moisture and nutrient status influence greenhouse gas fluxes from drained organic soils? Soil Biol. Biochem. 135, 71–84. https://doi.org/10.1016/j.soilbio.2019.04.013.

Šigut, L., 2021. Openeddy: The R package for low frequency eddy covariance data processing. R package version 0.0.0.9005.

Simek, M., Cooper, J.E., 2002. The influence of soil pH on denitrification: progress towards the understanding of this interaction over the last 50 years. Eur. J. Soil. Sci. 53, 345–354. https://doi.org/10.1046/j.1365-2389.2002.00461.x.

Šimůnek, J., Šejna, M., Saito, H., Sakai, M., van Genuchten, M.T., 2013. The HYDRUS-1D software package for simulating the one-dimensional movement of water, heat, and multiple solutes in variably-saturated media. Department of Environmental Sciences, University of California Riverside, California.

Smith, K.A., Thomson, P.E., Clayton, H., McTaggart, I.P., Conen, F., 1998. Effects of temperature, water content and nitrogen fertilisation on emissions of nitrous oxide by soils. Atmos. Environ. 32 (19), 3301–3309. https://doi.org/10.1016/S1352-2310(97)00492-5.

Tanneberger, F., Appulo, L., Ewert, S., Lakner, S., Ó Brolcháin, N., Peters, J., Wichtmann, W., 2021. The power of nature-based solutions: How peatlands can help us to achieve key EU sustainability objectives. Adv. Sustainable Syst. 5 (1), 2000146 https://doi.org/10.1002/adsu.202000146.

Tiemeyer, B., Albiac Borraz, E., Augustin, J., Bechtold, M., Beetz, S., Beyer, C., Drösler, M., Ebli, M., Eickenscheidt, T., Fiedler, S., Förster, C., Freibauer, A., Giebels, M., Glatzel, S., Heinichen, J., Hoffmann, M., Höper, H., Jurasinski, G., Leiber-Sauheitl, K., Peichl-Brak, M., Roßkopf, N., Sommer, M., Zeitz, J., 2016. High emissions of greenhouse gases from grasslands on peat and other organic soils. Global Change Biol 22 (12), 4134–4149. https://doi.org/10.1111/gcb.13303.

Tiemeyer, B., Freibauer, A., Borraz, E.A., Augustin, J., Bechtold, M., Beetz, S., Beyer, C., Ebli, M., Eickenscheidt, T., Fiedler, S., Förster, C., Gensior, A., Giebels, M., Glatzel, S., Heinichen, J., Hoffmann, M., Höper, H., Jurasinski, G., Laggner, A., Leiber-Sauheitl, K., Peichl-Brak, M., Drösler, M., 2020. A new methodology for organic soils in national greenhouse gas inventories: data synthesis, derivation and application. Ecol Indic 109, 105838. https://doi.org/10.1016/j.ecolind.2019.105838.

Tiemeyer, B., Kahle, P., 2014. Nitrogen and dissolved organic carbon (DOC) losses from an artificially drained grassland on organic soils. Biogeosciences 11 (15), 4123–4137. https://doi.org/10.5194/bg-11-4123-2014.

Tuittila, E.-.S., Vasander, H., Laine, J., 2004. Sensitivity of C sequestration in reintroduced sphagnum to water-level variation in a cutaway peatland. Restor. Ecology 12 (4), 483–493. https://doi.org/10.1111/j.1061-2971.2004.00280.x.

van den Akker, J.J.H., Jansen, P.C., Hendriks, R.F.A., Hoving, I., Pleijter, M., 2012. Submerged infiltration to halve subsidence and GHG emissions of agricultural peat soils. In: Proceedings of the 14th International Peat Congress. Stockholm, Sweden. Article 383.

van den Heuvel, R.N., Bakker, S.E., Jetten, M.S.M., Hefting, M.M., 2011. Decreased N_2O reduction by low soil pH causes high N_2O emissions in a riparian ecosystem. Geobiology 9 (3), 294–300. https://doi.org/10.1111/j.1472-4669.2011.00276.x.

van Genuchten, M.T., 1980. A closed-form equation for predicting the hydraulic conductivity of unsaturated soils. Soil Sci. Soc. Am. J. 44 (5), 892–898. https://doi.org/10.2136/sssaj1980.03615995004400050002x.

Frank, S., 2016. Factors controlling concentrations and losses of dissolved carbon and nitrogen from disturbed bogs in Lower Saxony (Germany). Dissertation, Hannover, 129 pp. doi:10.15488/8674.

UBA (German Environment Agency), 2021. Submission under the United Nations Framework Convention on Climate Change and the Kyoto Protocol 2021: National Inventory Report for the German Greenhouse Gas Inventory 1990 – 2019. Climate Change 44/2021, Dessau-Roßlau, Germany.

VDLUFA, 2011. Band II.1 Die Untersuchung von Düngemitteln, Darmstadt.

VDLUFA, 2012. Band I Die Untersuchung von Böden, Darmstadt.

Velthof, G.L., Hoving, I.E., Dolfing, J., Smit, A., Kuikman, P.J., Oenema, O., 2010. Method and timing of grassland renovation affects herbage yield, nitrate leaching, and nitrous oxide emission in intensively managed grasslands. Nutr. Cycl. Agroecosyst. 86 (3), 401–412. https://doi.org/10.1007/s10705-009-9302-7.

Wang, Y., Paul, S.M., Jocher, M., Alewell, C., Leifeld, J., 2022. Reduced nitrous oxide emissions from drained temperate agricultural peatland after coverage with mineral soil. Front. Environ. Sci. 10, 856599 https://doi.org/10.3389/fenvs.2022.856599.

Webb, E.K., Pearman, G.I., Leuning, R., 1980. Correction of flux measurements for density effects due to heat and water vapour transfer. Quart. J. R. Met. Soc. 106, 85–100. https://doi.org/10.1002/qj.49710644707.

Weideveld, S.T.J., Liu, W., van den Berg, M., Lamers, L.P.M., Fritz, C., 2021. Conventional subsoil irrigation techniques do not lower carbon emissions from drained peat meadows. Biogeosciences 18 (12), 3881–3902. https://doi.org/10.5194/bg-18-3881-2021.

Wen, Y., Freeman, B., Hunt, D., Musarika, S., Zang, H., Marsden, K.A., Evans, C.D., Chadwick, D.R., Jones, D.L., 2021. Livestock-induced N_2O emissions may limit the benefits of converting cropland to grazed grassland as a greenhouse gas mitigation strategy for agricultural peatlands. Resources, Conservation and Recycling 174, 105764. https://doi.org/10.1016/j.resconrec.2021.105764.

Weslien, P., Kasimir Klemedtsson, Å., Börjesson, G., Klemedtsson, L., 2009. Strong pH influence on N_2O and CH_4 fluxes from forested organic soils. Eur. J. Soil Sci. 60 (3), 311–320. https://doi.org/10.1111/j.1365-2389.2009.01123.x.

Wilczak, J.M., Oncley, S.P., Stage, S.A., 2001. Sonic Anemometer Tilt Correction Algorithms. Boundary-Layer Meteorol 99 (1), 127–150. https://doi.org/10.1023/A:1018966204465.

Wilson, D., Blain, D., Couwenberg, J., Evans, C.D., Murdiyarso, D., Page, S.E., Renou-Wilson, F., Rieley, J.O., Sirin, A., Strack, M., Tuittila, E.-.S., 2016. Greenhouse gas emission factors associated with rewetting of organic soils. Mires and Peat 17, 1–28. https://doi.org/10.19189/MaP.2016.OMB.222.

Wrage-Mönnig, N., Horn, M.A., Well, R., Müller, C., Velthof, G., Oenema, O., 2018. The role of nitrifier denitrification in the production of nitrous oxide revisited. Soil Biol. Biochem. 123, A3–A16. https://doi.org/10.1016/j.soilbio.2018.03.020.

Wutzler, T., Lucas-Moffat, A., Migliavacca, M., Knauer, J., Sickel, K., Šigut, L., Menzer, O., Reichstein, M., 2018. Basic and extensible post-processing of eddy covariance flux data with REddyProc. Biogeosciences 15 (16), 5015–5030. https://doi.org/10.5194/bg-15-5015-2018.

Wutzler, T., Reichstein, M., Moffat, A.M., Migliavacca, M., 2020. REddyProc: post processing of (Half-)hourly eddy-covariance measurements. R package version 1.2.2.